Uncovering the multifaceted mechanism of action of a historical antimicrobial

Oluwatosin Qawiyy Orababa[1*], Jessica Furner-Pardoe[1,8*], Alexander Gale[1], Blessing Anonye[1], Joe Ratcliff[1], Natasha Reddy[2], Ramón Garcia Maset[2,4], Niamh E. Harrington[1,5], Shajini Subhaskaran[1], Séamus Holden[1], Stephen P. Diggle[3,6], Christophe Corre[1,7], Freya Harrison[1,6]

[1] School of Life Sciences, Gibbet Hill Campus, University of Warwick, Coventry, CV47AL, United Kingdom

[2] Warwick Medical School, Gibbet Hill Campus, University of Warwick, Coventry, CV47AL, United Kingdom

[3] School of Biological Sciences, Georgia Institute of Technology, North Avenue, Atlanta, GA 30332, United States

[4] Centre for Urological Biology, Department of Renal Medicine, Division of Medicine, University College London, London, WC1E 6BT, UK (Current address)

[5] Institute of Infection, Veterinary and Ecological Sciences, University of Liverpool, L69 3BX, UK (Current address)

[6] Centre for Biomolecular Sciences, School of Life Sciences, University of Nottingham, University Park, Nottingham, United Kingdom

[7] Department of Chemistry, University of Warwick, Coventry, CV47AL, United Kingdom

[8] Department of Paleoniotechnology, Leibniz Institute for Natural Product Research and Infection Biology (Hans-Knöll Institute – Leibniz-HKI), Beutenbergstraße 11A, 07745 Jena, Thuringia, Germany (Current address)

*Equal contributors

Address correspondence to FH: f.harrison@warwick.ac.uk or OQO: Oluwatosin.orababa@warwick.ac.uk

ABSTRACT

Natural products have provided most of our modern pharmacopoeia, serving as active molecules or scaffolds for active molecules. Their use in drug development is often inspired by their traditional or historical medical use. For many decades, this discovery pipeline has

focused on identifying a single molecule responsible for much of the biological activity of a "raw" natural product preparation (e.g. a whole-plant extract) and scoping this molecule for clinical potential. However, it is increasingly realised that historical/traditional remedies with significant biological activity may owe this activity to the combined action of multiple molecules. Concomitantly, microbiologists increasingly argue that effectively fighting antimicrobial-resistant infections will rely on combination therapies that combine multiple antimicrobials and/or adjuvant molecules. We previously reconstructed a complex historical remedy, Bald's eyesalve. Our reconstruction of this remedy had strong antibiofilm activity, which relied on the presence of multiple ingredients. Here, we report that Bald's eyesalve has multiple mechanisms of action against exemplar Gram-positive (*Staphylococcus aureus*) and Gram-negative (*Acinetobacter baumannii*) pathogens. Bald's eyesalve depolarises and permeabilises the plasma membrane, and the Gram-negative outer membrane; inhibits expression of bacterial adhesins, virulence factors and efflux pumps in both *S. aureus* and *A. baumannii*; inhibits quorum sensing in *S. aureus*; and causes downregulation of genes involved in *de novo* nucleotide biosynthesis in *S. aureus*. Lastly, we show that this multifaceted mechanism of action makes it difficult for *S. aureus*, *A. baumannii*, and *Pseudomonas aeruginosa* to evolve resistance against Bald's eyesalve. Bald's eyesalve could be used to identify a defined cocktail of natural products suitable for preclinical testing as a multi-target antibacterial preparation to which resistance may arise more slowly than current single-molecule antibiotics.

Importance

The increasing mortality and economic cost of antimicrobial resistance (AMR) have made it one of the biggest threats to global health. Available antibiotics are in short supply due to the slow progress in the discovery of new antibiotics. Hence, there is a need for alternative treatment options against difficult-to-treat infections. We have identified a natural product cocktail based on a historical remedy with broad-spectrum antibacterial activity and a multifaceted mechanism of action. We have shown that there is slower resistance evolution to this cocktail compared to mainline antibiotics, and it could be used as the foundation of an alternative treatment to antibiotics in clinical settings.

KEYWORDS

AMR, Ancientbiotics, Antibiotic mechanisms, Antivirulence mechanisms, Biofilm, Natural products

INTRODUCTION

In 2021 alone, bacterial antimicrobial resistance (AMR) was associated with 4.71 million deaths (Naghavi *et al.,* 2024). If this silent pandemic of increasing AMR persists, close to 170 million lives will be lost to AMR-associated infections between 2025 and 2050 (Naghavi *et al.,* 2024). AMR is costly in economic terms as wells in human lives lost in 2019, total hospital costs and productivity loss associated with AMR infections were close to USD700 bn and USD200 bn, respectively (Naylor *et al.,* 2025). The twin challenges of selective pressure for resistance to mainline antibiotics (Ahmed *et al.,* 2024) and the scarcity of new antimicrobial treatments in the clinical pipeline (Kavanagh, 2025; Prasad *et al.,* 2022) create an urgent need to find novel therapies with a long clinical shelf life in the face of bacterial abilities to rapidly mutate and adapt.

Increasingly, researchers are hunting for antibacterial agents whose mechanism of action involves attacking multiple cellular targets, and/or that target bacterial structures or functions that are highly evolutionarily conserved, such as the cell membrane. Combination therapies, which comprise two or more active compounds, or which combine active compounds with adjuvants that enhance their activity, are increasingly recognised as one way to achieve this aim (Woods and Read, 2023; Si *et al.,* 2023). Combination therapies may range from a simple combination of an antibiotic plus a molecule that reduces the ability of bacteria to evade antibiotic attack (e.g. beta-lactam plus beta-lactamase inhibitor) to a chemically complex preparation (e.g. medical-grade honey, which uses several mechanisms to kill bacteria and to which it appears to be hard for bacteria to evolve resistance) (Yahav *et al.,* 2020; Ogwu and Izah, 2025).

Our modern clinical use of honey stems from its long history of use in traditional and “folk” medicine around the world (Sharaf El-Din *et al.,* 2025; Eteraf-Oskouei and Najafi, 2013). Ethnopharmacology and interdisciplinary studies of historical medicine thus have the potential to identify natural products with clinically-significant antibacterial activity. Focussing on plants and plant-derived preparations, it is now clear that many plant extracts contain not just individual compounds with strong antibacterial activity and a promising therapeutic index (Muhs *et al.,* 2017), but combinations of compounds that act additively or synergistically to produce a high level of antibacterial activity (Caeser and Cech, 2019). A

textbook example of a single-molecule antimicrobial compound derived from a plant used in historical medicine is the antimalarial drug artemisinin (Tu, 2011): however, more recent research has shown that complex extracts of the parent plant have more potent antimicrobial activity than purified artemisinin (Gruessner *et al.,* 2019).

We and our collaborators in the Ancientbiotics consortium (Connelly *et al.,* 2022) previously explored the antibacterial potential of a historical remedy known as Bald's eyesalve, from an early medieval English medical text called Bald's Leechbook (Harrison *et al.,* 2015; Furner-Pardoe *et al.,* 2020; Anonye *et al.,* 2020). This multi-part natural product remedy was made by combining garlic (*Allium sativum*), another *Allium* species (we explored onions or leek, *A. cepa* / *A. ampeloprasum*), wine, and bovine bile, and was used to treat a "lump" in the eye, which we interpreted as likely a stye - caused by bacterial infection of an eyelash follicle. Our version of Bald's eyesalve has been shown to have significant antibacterial efficacy in *in vitro* wound biofilm models and in biofilm-containing biopsies from mice with chronic wound infections. We confirmed that optimal antibiofilm efficacy of this complex natural product remedy was only seen when all ingredients were combined, consistent with synergistic and/or additive interactions existing between the ingredients (Harrison *et al.,* 2015; Furner-Pardoe *et al.,* 2020), and showed broad-spectrum activity against several Gram-positive and Gram-negative species (Furner-Pardoe *et al.,* 2020). Preclinical safety testing revealed no serious adverse effects of the reconstructed Bald's eyesalve *in vitro* or *in vivo* (Anonye *et al.,* 2020; Bruce *et al.,* 2022).

In this study, we first confirmed that the antibacterial efficacy of Bald's eyesalve against selected priority pathogens is replicated in different infection-mimicking growth environments. We then used phenotypic assays and transcriptomics to unravel the mechanism of action of Bald's eyesalve against *Staphylococcus aureus* and *Acinetobacter baumannii* (WHO priority pathogens for new drug development, with a high AMR-associated mortality burden (Murray *et al.,* 2022; Naghavi *et al.,* 2024). We found that the eyesalve has a multifaceted mechanism of action, with multiple targets - some of which were unique to one of the two species studied, and some of which were shared. We then used laboratory selection experiments to select *S. aureus*, *A. baumannii*, and *P. aeruginosa* for resistance to the eyesalve, or to commonly-used antibiotics. We found that while all bacteria rapidly evolved high-level resistance to antibiotics, they were unable to evolve resistance to the eyesalve.

Bald's eyesalve could therefore contain an identifiable cocktail of natural products suitable for development into a multi-target antibacterial preparation with clinical potential.

RESULTS

Bald's eyesalve has good antibacterial activity against *S. aureus, A. baumannii,* and *P. aeruginosa* strains in infection-mimicking media

We have previously shown that Bald's eyesalve has potent antimicrobial and antibiofilm activity against a range of bacterial pathogens, and that using onion, rather than leek, as the second *Allium* species gives more consistent activity between batches (Furner-Pardoe *et al.,* 2020). We prepared fresh batches of eyesalve from garlic, onion, wine, and bovine bile and carried out broth microdilution assays to calculate the minimum inhibitory concentration (MIC) against representative lab strains (*S. aureus*, *A. baumannii*, and *P. aeruginosa*) - WHO priority pathogens that cause AMR infections in chronic wounds and cystic fibrosis (CF) lungs. The assays were repeated in a standard lab medium (cation-adjusted Mueller-Hinton broth, caMHB) and in two infection-mimicking media - simulated wound fluid (SWF) (Werthén *et al.,* 2010) and synthetic cystic fibrosis sputum media (SCFM) (Palmer *et al.,* 2007). The host-mimicking media were used because minimum inhibitory concentrations (MICs) of antimicrobials in standard lab media often do not accurately predict *in vivo* activity (Ersoy *et al.,* 2017; Furner-Pardoe *et al.,* 2020; Sweeney *et al.,* 2020)

As shown in Table 1, and consistent with previous results (Furner-Pardoe *et al.,* 2020), Bald's eyesalve showed good antibacterial efficacy against all these pathogens in both standard lab and infection-mimicking media. Also consistent with previous results, the MIC for *S. aureus* USA300, an MRSA strain, was higher than its MIC against *S. aureus* Newman, a methicillin-susceptible strain; and the highest MIC was seen against *P. aeruginosa* in both caMHB and SWF. Interestingly, in SCFM, Bald's eyesalve showed better inhibitory activity against a *P. aeruginosa* strain derived from an epidemic cystic fibrosis clone (LESB58) compared to *P. aeruginosa* PA14. In SCFM, both *A. baumannii* AT6619606 and the highly virulent strain 50575 had the same MIC.

Table 1. Antibacterial activity of Bald's eyesalve against *S. aureus, A. baumannii,* and *P. aeruginosa* in different media. Two strains of *S. aureus* (one MSSA lab strain, Newman, and one MRSA derived from an epidemic pneumonia clone,

USA300 LAC) and one lab strain each of *A. baumannii* and *P. aeruginosa* were assayed in the standard antibiotic susceptibility testing medium, caMHB. The same four strains were assayed in synthetic wound fluid (SWF) as all three species are common wound pathogens. For assays in synthetic cystic fibrosis sputum medium (SCFM), we focused on *A. baumannii* and *P. aeruginosa*, including the laboratory strains tested in caMHB and SWF, and added an example highly virulent strain of each species.

	caMHB			
MIC (% v/v)	***S. aureus* Newman**	***S. aureus* USA300 LAC**	***P. aeruginosa* PA14**	***A. baumannii* ATCC1966**
	3.13	6.25	25.00	3.13
	SWF			
MIC (% v/v)	***S. aureus* Newman**	***S. aureus* USA300 LAC**	***P. aeruginosa* PA14**	***A. baumannii* ATCC1966**
	6.25	12.50	25.00	6.25
	SCFM			
MIC (% v/v)	***P. aeruginosa* PA14**	***P. aeruginosa* LESB58**	***A. baumannii* ATCC1966**	***A. baumannii* 5075**
	12.50	3.13	0.78	0.78

Bald's eyesalve causes depolarisation and permeabilisation of the bacterial plasma membrane, and permeabilisation of the Gram-negative outer membrane

We first assessed whether Bald's eyesalve had any effect on bacterial membrane integrity or function. The mixture contains bile salts, which cause pore formation in membranes (Garidel *et al.,* 2007), and allicin, which is derived from garlic and onion and is known to interact with membranes and affect their integrity (Gruhlke *et al.,* 2015). Ethanol and organic acids, typically present in wine, are also known to affect membrane function (Ji *et al.,* 2023; Loison

et al., 2016). Several assays were carried out on bacteria treated with Bald's eyesalve for a short period (1-2h).

The impact of Bald's eyesalve on the plasma membrane potential of lab strains of *S. aureus* (MSSA), *A. baumannii*, and *P. aeruginosa* was assessed with the dye DiSC3(5), which accumulates in the membrane and alters its fluorescence in response to changes in electric potential (Buttress *et al.*, 2022). For all three species, we observed an increase in the fluorescence of DiSC3(5) upon the addition of Bald's eyesalve, which was not seen with the control treatment (sterile water) (FIG 1A). This is an indication of membrane potential disruption via depolarisation.

Some antibiotics, like polymyxins, have dual membrane activity, both depolarising and permeabilising the membrane. To assess if Bald's eyesalve also permeabilises the plasma membrane, we used propidium iodide (PI). PI is a membrane-impermeable nucleic acid dye whose fluorescence increases when bound to the nucleic acid of a membrane-damaged cell. There was increased fluorescence when PI was added to Bald's eyesalve-treated cells compared to untreated cells, indicating membrane damage in response to Bald's eyesalve (FIG 1B).

To further confirm plasma membrane perturbation in response to Bald's eyesalve, we stained Bald's eyesalve-treated (at 2×MIC) *S. aureus* and *A. baumannii* with the plasma membrane stain FM4-64. For *S. aureus*, we observed a bulging morphology (red arrows), which was better seen in the phase contrast channel and increased FM4-64 fluorescence (indicating membrane perturbation; blue arrows) in Bald's eyesalve-treated cells, which was not seen in the control cells (FIG 1C). With *A. baumannii*, we also observed morphological changes (presence of dense spots of fluorescence) indicative of membrane perturbation (blue arrows) (FIG 1C).

Finally, we assessed if Bald's eyesalve caused any significant damage to the Gram-negative outer membrane or Gram-positive cell wall by imaging *A. baumannii* and *S. aureus* treated with Bald's eyesalve with a scanning electron microscope (SEM) (FIG 2). This revealed the presence of deformations in the outer membranes of Bald's eyesalve-treated *A. baumannii* cells, which were absent in untreated cells. We did not observe any obvious change in the surface morphology of *S. aureus* under similar treatment, suggesting the cell wall remained

largely intact (FIG 2). Negative stain transmission electron microscopy (TEM) was therefore used for *S. aureus* only, and this confirmed that while the cell wall of *S. aureus* was not affected by Bald's eyesalve treatment, there was observable wrinkling and deformation of the plasma membrane, consistent with the results of the various assays described above (FIG 3). For comparison, *S. aureus* treated with antibiotics that either induce membrane pore formation (nisin) or inhibit cell wall synthesis (vancomycin) were also imaged under negative stain TEM; the effect of eyesalve was not visually comparable to that of either antibiotic.

Transcriptomic analysis reveals multiple intracellular responses of *S. aureus* and *A. baumannii* to Bald's eyesalve, indicating that oxidative stress and DNA damage are part of its mechanism of action

Gene expression analysis using RNA sequencing provides insights into both the primary potential targets and downstream responses to a drug (Szalai and Veres, 2023; Hudson and Lockless, 2022). To understand gene expression changes in response to Bald's eyesalve, we carried out RNA sequencing of *S. aureus* and *A. baumannii* treated with 2×MIC of Bald's eyesalve for 2 h. The cost of RNA sequencing prevented this analysis from being carried out on *P. aeruginosa*. The dose and time point were chosen based on the changes observed with the FM4-64 membrane staining of *S. aureus* and *A. baumannii* treated with 2×MIC of Bald's eyesalve for 2 h (FIG 1C). FIG 4 shows the significantly enriched gene ontology groups of the top 100 differentially upregulated and downregulated genes in *S. aureus* and *A. baumannii*. Significantly differentially expressed genes were defined as those with p-values < 0.05 and $|\log2\text{foldchange}| \geq 1.5$ in treated vs. untreated samples. Overall, more GO groups were significantly enriched in *S. aureus* than in *A. baumannii*.

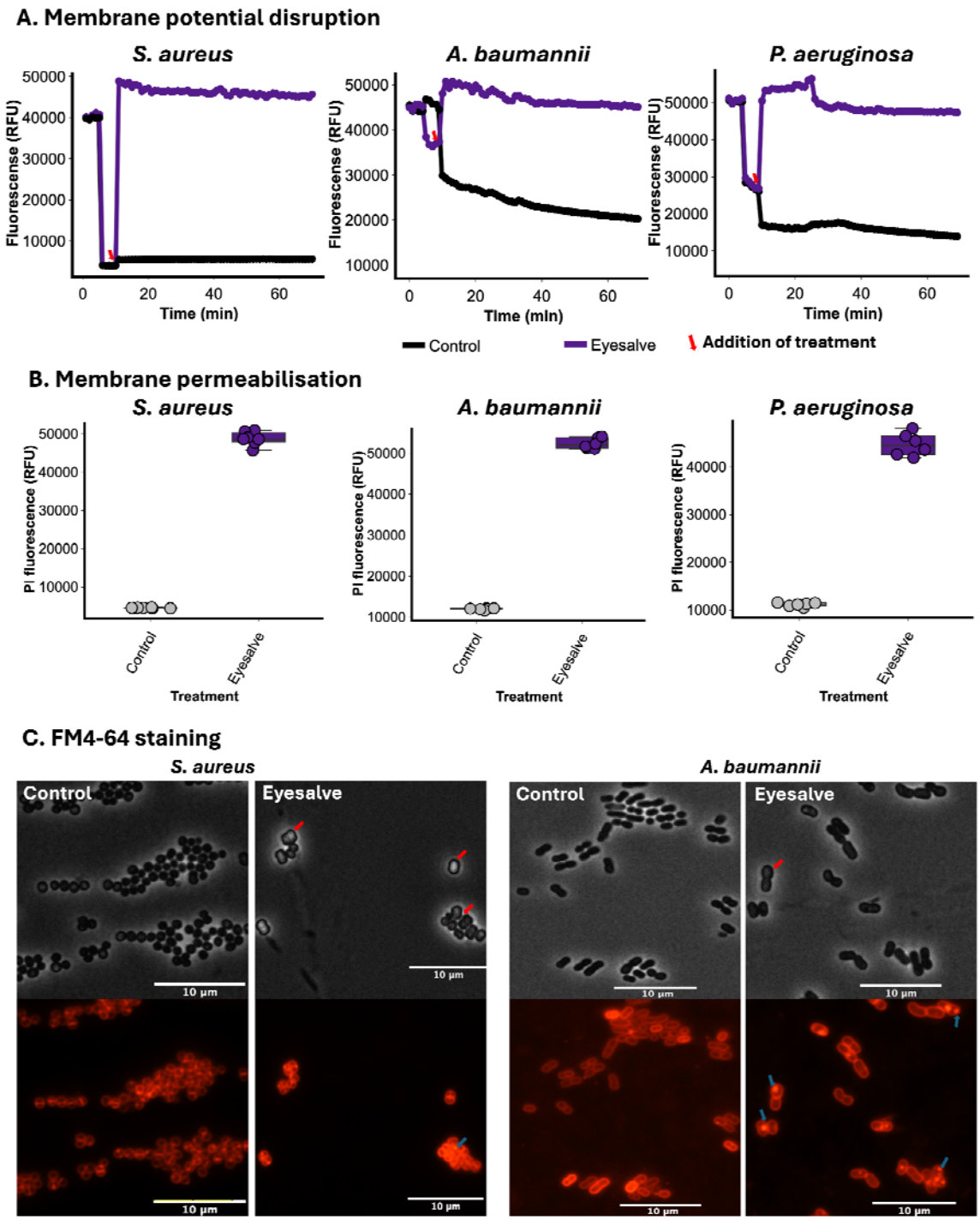

FIG 1. Bald's eyesalve disrupts the bacterial plasma membrane. A. *S. aureus* Newman, *A. baumannii* ATCC 19606, and *P. aeruginosa* PA14 were stained with DiSC3(5), treated with either 1×MIC of Bald's eyesalve (purple) or water (black), and their fluorescence monitored for 1 h. There was increased DiSC3(5) fluorescence, indicating membrane depolarisation in samples treated with Bald's eyesalve. The red arrow indicate point of treatment. Each line represents the mean of three technical

replicates. **B.** *S. aureus* Newman, *A. baumannii* ATCC 19606, and *P. aeruginosa* PA14 were treated with 1×MIC of Bald's eyesalve (purple) or water (grey) for 1 h, stained with propidium iodide, and fluorescence was measured after 1 h. Each symbol represents an individual bacterial culture; box plots show the fluorescence intensity (in RFU) of propidium iodide. **C.** *S. aureus* Newman and *A. baumannii* ATCC 19606 were treated with 2×MIC of Bald's eyesalve or water for 2 h, stained with FM4-64, and then imaged with a widefield fluorescence microscope at oil immersion lens (x100) magnification. Increased FM4-64 fluorescence in *S. aureus* and the presence of dense spots of fluorescence in *A. baumannii* suggest membrane perturbation.

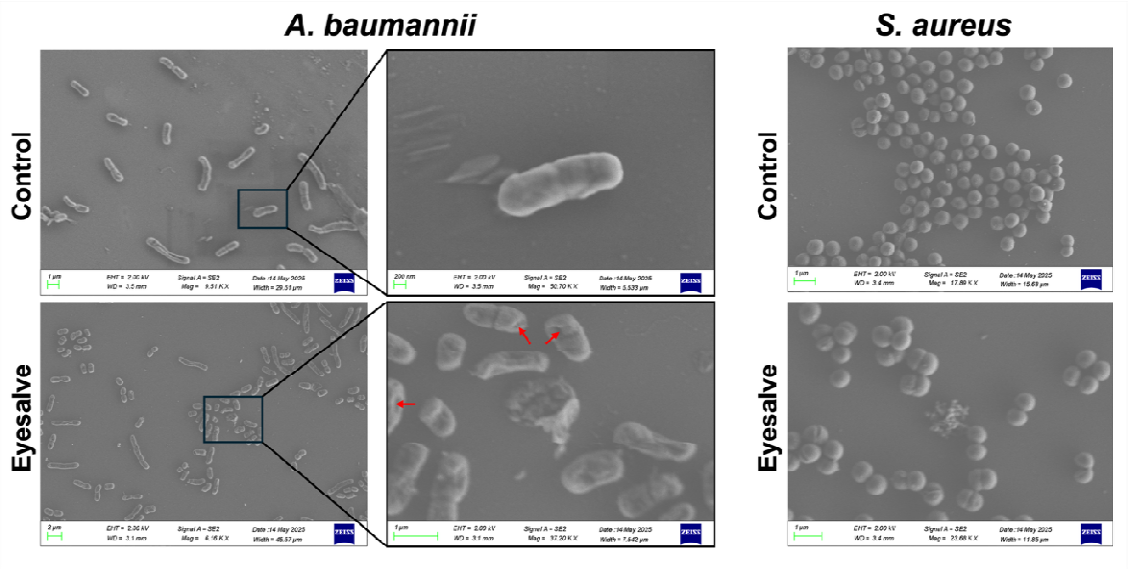

FIG 2. Bald's eyesalve caused observable deformation on the outer membrane of *A. baumannii*. Both *A. baumannii* ATCC 19606 and *S. aureus* Newman were treated with 2×MIC of Bald's eyesalve or water for 2 h and imaged with a scanning electron microscope.

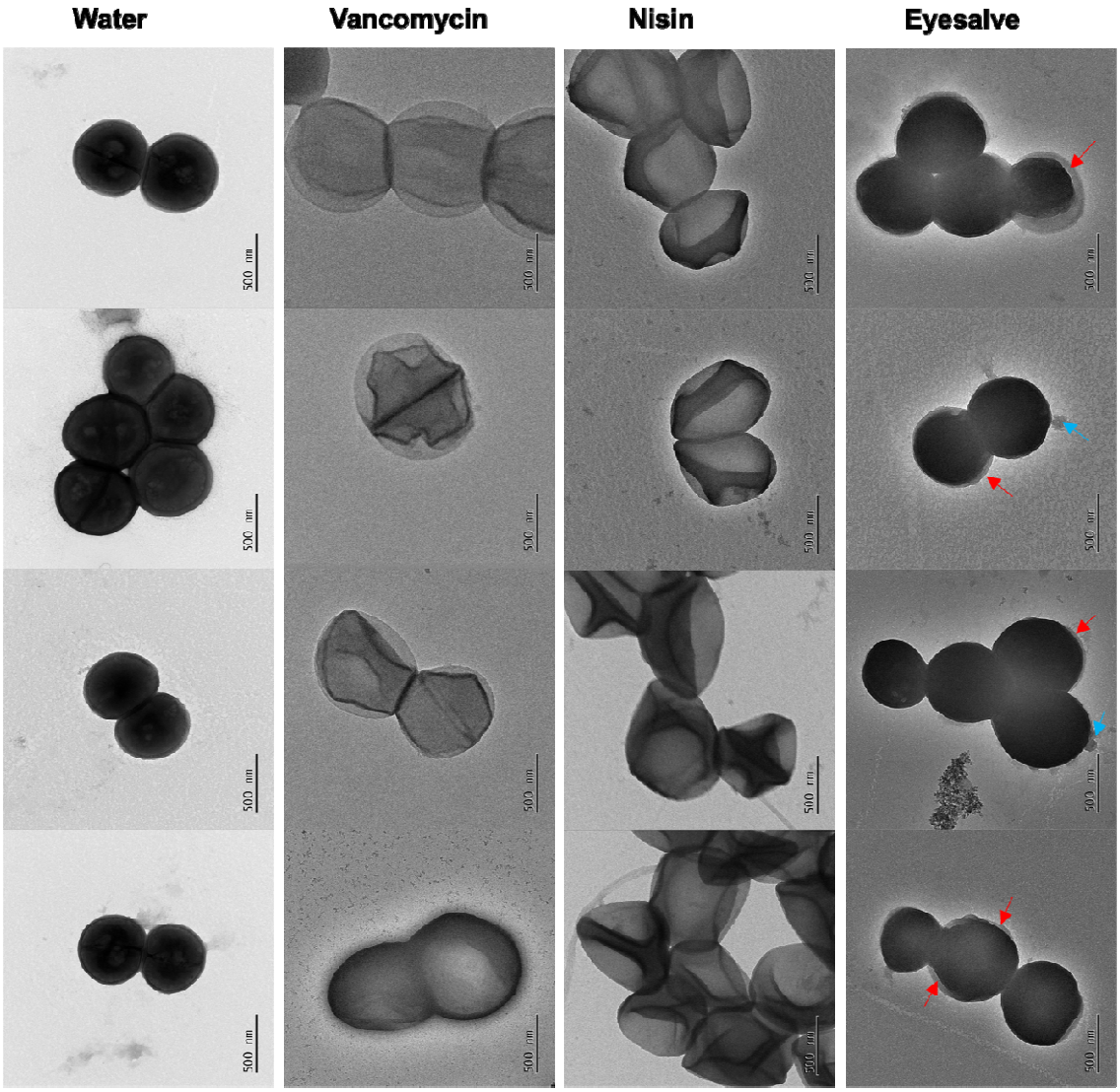

FIG 3. Bald's eyesalve caused the deformation of *S. aureus* inner membrane. *S. aureus* Newman was treated with water, Bald's eyesalve (100%), nisin (150 µg/ml), or vancomycin (100 µg/ml) for 4 h. Treated cells were negatively stained using ELMO glow discharge and uranium acetate. The samples were then imaged using a transmission electron microscope.

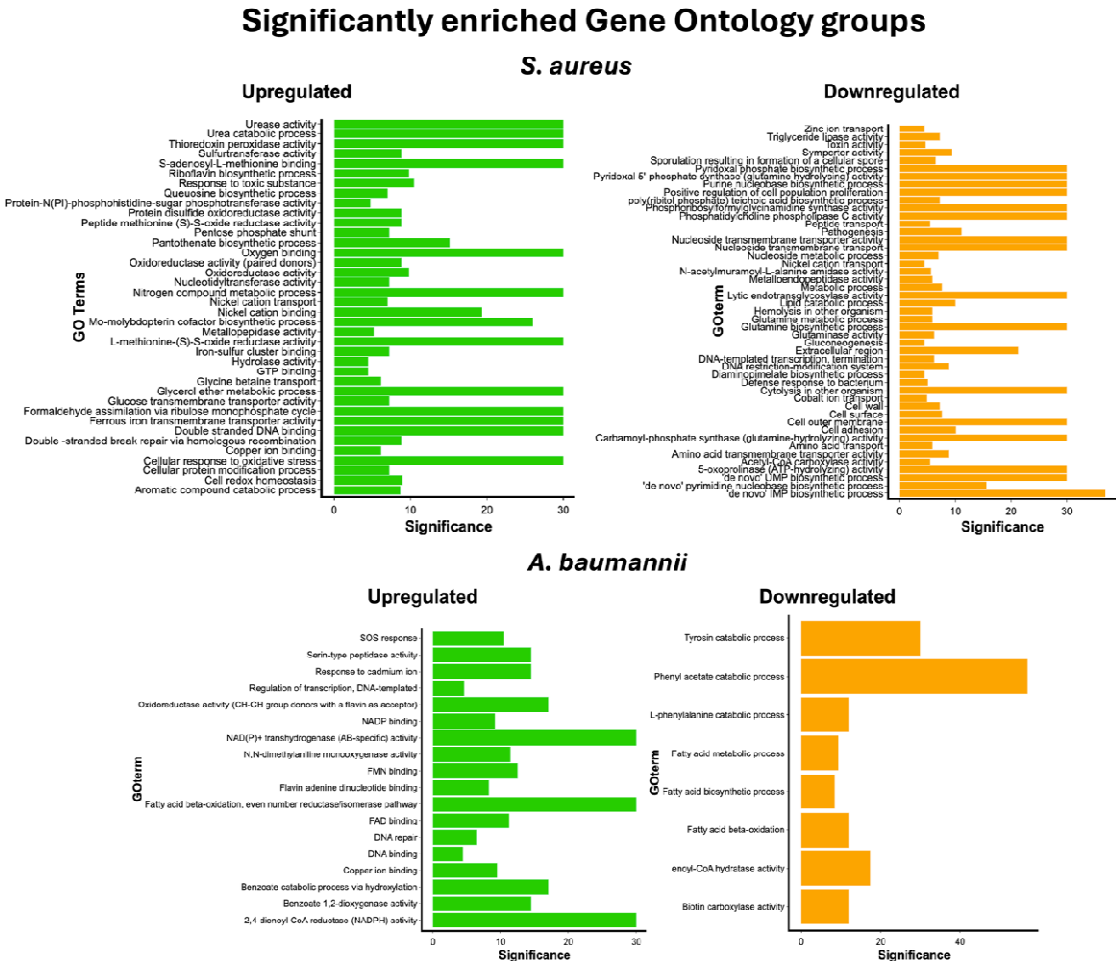

FIG 4. Significantly upregulated and downregulated gene ontology groups in *S. aureus* and *A. baumannii* in response to 2h treatment of 2×MIC of Bald's eyesalve. Significantly differentially expressed genes were defined as those with p-values ≤ 0.05 and |log2foldchange| ≥1.5 in treated vs. untreated samples; n = 3 and 4 cultures per treatment for *A. baumannii* ATCC 19606 and *S. aureus* Newman, respectively.

In *S. aureus*, GO groups with significant changes in expression included "cell outer membrane", "cell surface" and "cell wall", consistent with the membrane effects shown in phenotypic assays. Membrane-related GO terms were not significantly represented in the response of *A. baumannii*, but upregulation of GO terms associated with cation transport in both species, including "copper ion binding", "ferrous iron transported activity" and "nickel cation transport/binding", might be associated with downstream effects of membrane depolarisation.

We also observed significant downregulation of the GO term “pathogenesis”. Notable among these genes are the alpha hemolysin (*hla*), bicomponent leukocidins (*lukGH*), and cysteine histidine amidohydrolase/peptidase (CHAP) domain-containing protein of staphylococcal secretory antigen (*ssaA1*) (Supplementary Table 1). These are important virulence factors produced by *S. aureus* during infections (Wang *et al.,* 2024; Zhu *et al.,* 2023).

Changes in *S. aureus* expression of “cell redox homeostasis”, “cellular response to oxidative stress”, “oxygen binding”, “oxidoreductase activity” and similar terms appear consistent with the known oxidising ability of allicin (Borlinghaus *et al.,* 2014), which we have shown to be present in the remedy in micromolar amounts (Furner-Pardoe *et al.,* 2020). This property allows allicin to damage proteins and DNA (Borlinghaus *et al.,* 2014); DNA damage is also indicated by the upregulation of GOs associated with DNA repair in both *S. aureus* (“double-stranded DNA binding” and “double-stranded DNA repair”) and *A. baumannii* (“DNA binding”, “DNA repair”), and by the upregulation of “SOS response” in *A. baumannii* (Supplementary Table 2).

Gene enrichment analysis also revealed the significant downregulation of genes involved in *de novo* purine and pyrimidine biosynthesis in *S. aureus* (“*de novo* UMP biosynthetic process”, “*de novo* IMP biosynthetic process”, “*de novo* pyrimidine nucleobase biosynthetic process”, and “purine nucleobase biosynthetic process”) (FIG 5). These pathways are essential in the biosynthesis of DNA, RNA, and second messengers, including c-di-GMP (Goncheva *et al.,* 2022). The downregulation of genes involved in purine and pyrimidine biosynthesis has previously been linked to increased antibiotic susceptibility and reduced virulence in *S. aureus* (Stevens *et al.,* 2025; Liu *et al.,* 2022). We also observed the significant downregulation of *pyrP*, which is involved in the pyrimidine salvage pathway, under the “cell outer membrane” GO group.

In *A. baumannii*, gene enrichment revealed a significant downregulation of GO terms associated with fatty acid metabolism (“fatty acid metabolic process”, “fatty acid biosynthetic process”, “fatty acid beta oxidation”, and “enoyl-CoA hydratase activity”). Fatty acid biosynthesis is important in plasma membrane and lipopolysaccharide biosynthesis in Gram-negative pathogens, and a decrease in its production has been associated with reduced risk of persistence in *A. baumannii* (Vergoz *et al.,* 2024). This also aligns with the membrane damage previously reported in FIG 1.

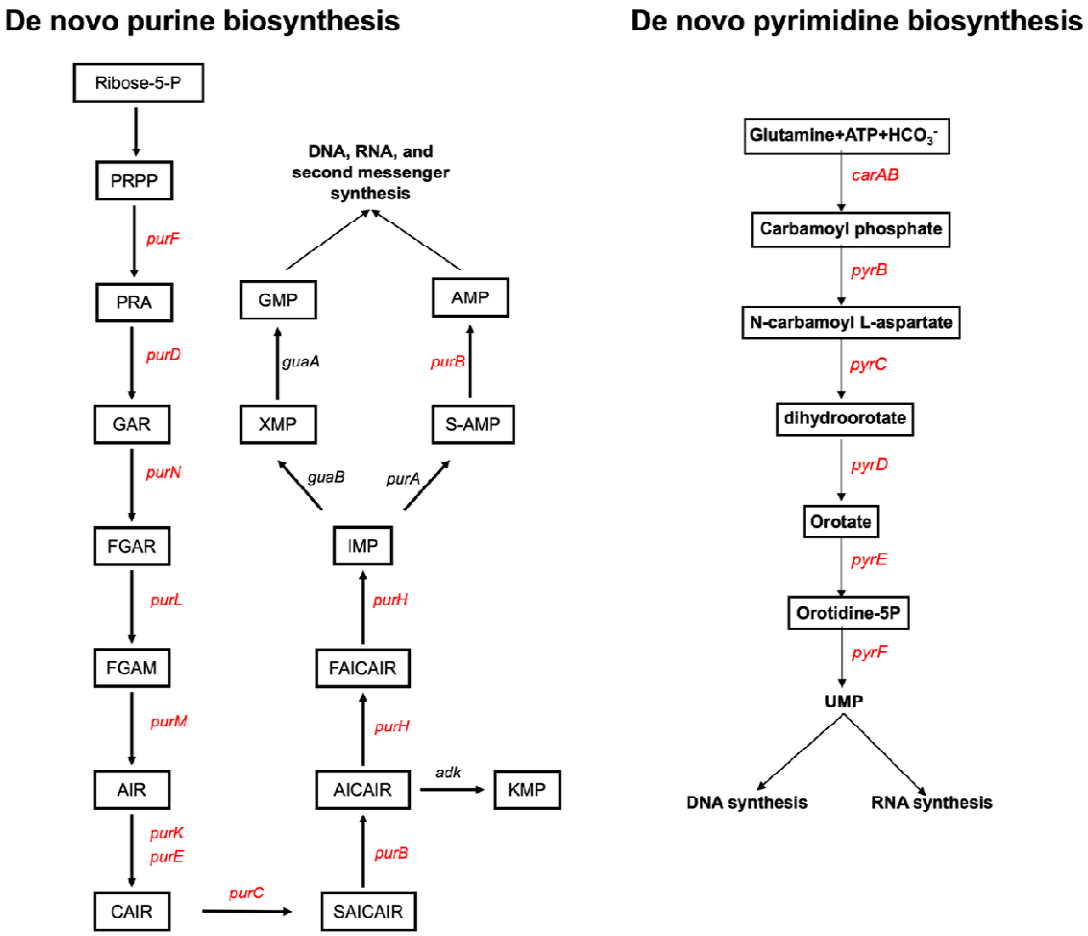

FIG 5. Bald's eyesalve inhibits *de novo* purine and pyrimidine biosynthesis in *S. aureus* Newman. Representation of the purine and pyrimidine *de novo* biosynthesis pathways in *S. aureus* Newman. Genes in red are significantly downregulated in *S. aureus* Newman in response to Bald's eyesalve. Significantly downregulated genes were defined as those with p-values ≤ 0.05 and log2foldchange ≤ -1.5 in treated vs. untreated samples; n = 4 cultures per treatment (PRPP = Phosphoribosyl pyrophosphate, PRA = phosphoribosylamine, GAR = glycinamide ribonucleotide, FGAR = phosphoribosylformylglycinamide, FGAM = formylglycinamidine ribonucleotide, AIR = aminoimidazole ribotide, CAIR = carboxyaminoimidazole ribonucleotide, SAICAIR = succinylaminoimidazole carboxamide ribonucleotide, AICAIR = aminoimidazole carboxamide ribonucleotide, FAICAIR = formaminoimidazole carboxamide ribonucleotide, IMP = inosine monophosphate,

XMP = xanthosine monophosphate, GMP = guanosine monophosphate, AMP = adenosine monosphosphate, UMP = uridine monophosphate).

Bald's eyesalve inhibits biofilm formation

The ability to inhibit biofilm formation would be a very useful property of an antimicrobial given in the early stages of infection, or in prophylactic applications such as functionalised wound dressings. Further, we have previously shown that Bald's eyesalve has strong antibiofilm activity against both *S. aureus* Newman and *A. baumannii* ATCC 19606. Therefore, we explored the dataset of DEGs to focus on genes involved in biofilm formation, although this group did not explicitly appear in the lists of significantly enriched GO terms for either species.

In *S. aureus*, some genes involved in biofilm formation (*sdrC, sdrD, sdrE,* and *cflB*) were differentially expressed and grouped under the GO term for "cell adhesion". Overall, only genes involved in the attachment stage of biofilm formation in *S. aureus* were differentially downregulated (FIG 6A). Other biofilm-associated genes, including those involved in biofilm matrix polysaccharide (the *ica* genes) and proteins (*fnbA* and *fnbB*) production, were slightly upregulated.

The majority of the biofilm-associated genes in *A. baumannii,* including genes responsible for the production of the biofilm exopolysaccharide, poly-N-acetyl glucosamine (PNAG) (*pgaABCD*), pili - for attachment (*csu* genes), and biofilm-associated proteins in *A. baumannii* (*bap*), were significantly downregulated. Additionally, there was significant downregulation of *bmfRS*, a major regulator of pili and biofilm polysaccharide production in *A. baumannii* (FIG 6B).

All our previous data showed that Bald's eyesalve kills bacteria in an established biofilm (Furner-Pardoe *et al.*, 2020), so we confirmed with *S. aureus* Newman that this remedy also inhibits biofilm formation (Supplementary FIG 1). This aligns with the downregulation of genes involved with attachment in *S. aureus*.

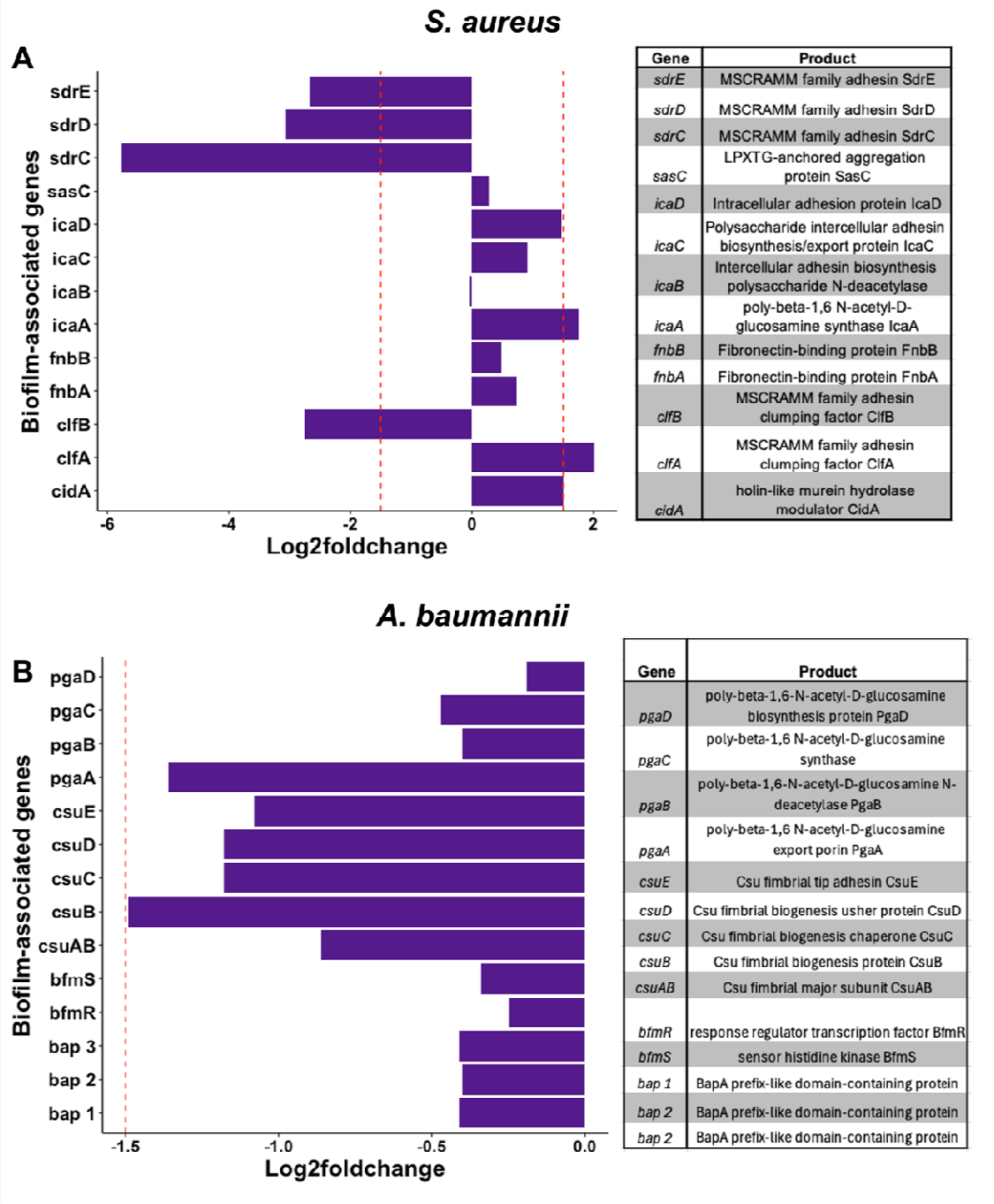

FIG 6. Bald's eyesalve inhibits biofilm formation in *S. aureus*. A. Expression profile of significantly differentially expressed ($p < 0.05$) biofilm-associated genes in *S. aureus* Newman in response to Bald's eyesalve. Red dashed lines indicate |log2-fold change| = 1.5, n = 4 cultures per treatment. B. Expression profile of significantly differentially expressed ($p < 0.05$) biofilm-associated genes in *A. baumannii* ATCC

19606 in response to Bald's eyesalve. Red dashed line indicates log2-fold change = -1.5, n = 3 cultures per treatment.

Bald's eyesalve represses quorum sensing in *S. aureus*

Due to the biofilm inhibitory effect of Bald's eyesalve on *S. aureus* and the inhibition of virulence factor expression, including alpha toxin (Hla), we decided to explore the expression profile of *agr* genes in *S. aureus*. The *S. aureus* Agr quorum-sensing system plays a significant role in controlling biofilm formation and virulence factor expression (FIG 7A). Transcriptomic analysis revealed the downregulation of *agrA*, *agrC*, and *agrB* in response to Bald's eyesalve (FIG 7A). AgrB processes a precursor of the auto-inducing peptide (AIP) signal, encoded by *agrD*, and exports the mature signal from the cell. AgrC and AgrA form a two-component system that senses extracellular AIP and, once the quorum is reached, activates transcription of both the *agrACDB* operon and of RNAIII, which in turn regulates loci controlling biofilm formation and virulence factor expression (FIG 7A).

To phenotypically confirm the repression of Agr-mediated quorum sensing by Bald's eyesalve, we assessed the effect of sub-inhibitory concentrations of Bald's eyesalve on two bioreporter strains: a constitutive reporter encoding GFP and a lux cassette under the control of a growth-dependent promoter (P_{xylA}:gfp:lux), and an AIP-dependent reporter containing the same construct under the control of the RNAIII promoter (P3:*gfp*:l*uxCDABE*) (Qazi *et al.*, 2001). We observed concentration-dependent quorum-sensing inhibition of the AIP-dependent reporter at low sub-inhibitory concentrations of Bald's eyesalve (1/100 and 1/1000 dilutions), which was not observed in the growth-dependent reporter (FIG 7B). A slightly higher sub-inhibitory concentration (1/10) caused a reduction in reporter expression from both promoters, consistent with this concentration causing general cellular stress as outlined above. The same pattern of inhibition against quorum-sensing reporters was also observed with the leek variant of Bald's eyesalve (Furner-Pardoe *et al.*, 2020).

Quorum-sensing reporters were not available for *A. baumannii*, but they are available for the other Gram-negative species explored phenotypically in this study, *P. aeruginosa*. In an experimental analogous to that described for *S. aureus*, we found that Bald's eyesalve did not affect the *las* (3-oxo-C12 homoserine lactone-mediated) quorum-sensing system, which positively regulates acute virulence in this species (Supplementary Fig 3).

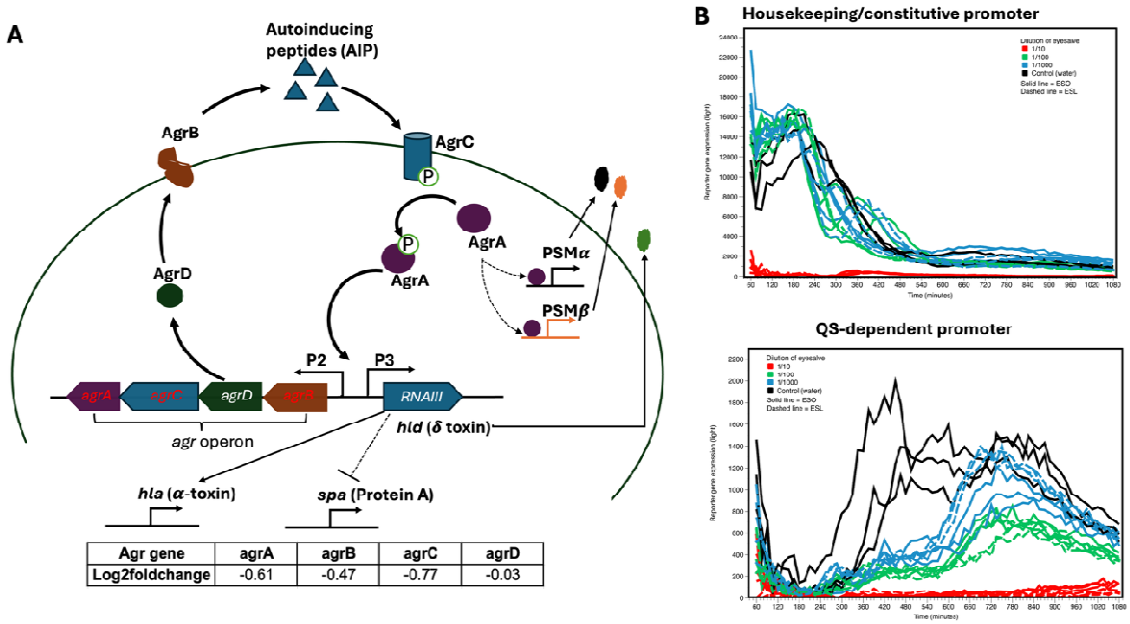

Agr gene	agrA	agrB	agrC	agrD
Log2foldchange	-0.61	-0.47	-0.77	-0.03

FIG 7. Bald's eyesalve inhibits quorum-sensing signalling in *S. aureus*. A. Downregulation of the expression of *agrA*, *agrB*, and *agrC*, which are involved in both quorum-sensing and virulence factor production in *S. aureus*. B. *S. aureus* growth-dependent/constitutive reporter (RN6390 S10:gfp:lux) and quorum-sensing/AIP-dependent reporter (RN6390 P3:gfp:lux) were exposed to sub-inhibitory concentrations (1/10, 1/100, and 1/1000) of Bald's eyesalve, or to sterile water, for 18 h and luminescence measured at intervals to assess the effect on quorum sensing. There was concentration-dependent repression of the reporter gene in the AIP-dependent reporter, shown by the peak of lux luminescence becoming progressively lower and later. ESO and ESL represent onion and leek variants of Bald's eyesalve, respectively. Each line represents an individual bacterial culture.

A model for the multifaceted mechanism of action of Bald's eyesalve on Gram-positive and Gram-negative bacteria

As shown in (FIG 8), Bald's eyesalve has a multifaceted mechanism of action, including a dual membrane activity and multiple intracellular activities. Bald's eyesalve disrupts the plasma membrane potential via depolarisation and permeabilises the membrane in both *S. aureus* and *A. baumannii*. It does not appear to cause noticeable structural damage to the *S. aureus* cell wall. In *A. baumannii*, Bald's eyesalve also permeabilises the outer membrane. Other activities of Bald's eyesalve include: inhibition of *S. aureus* quorum-sensing signalling by inhibiting the expression of *agrA*, *agrB*, and *agrC* genes, with concomitant inhibition of the expression of virulence factors; inhibition of nucleic acid biosynthesis by inhibiting *de*

novo purine and pyrimidine biosynthesis; and inhibition of biofilm formation by inhibiting the expression of adhesins in both *S. aureus* and *A. baumannii*; Inhibition of efflux pumps in both *S. aureus* and *A. baumannii* (FIG 8).

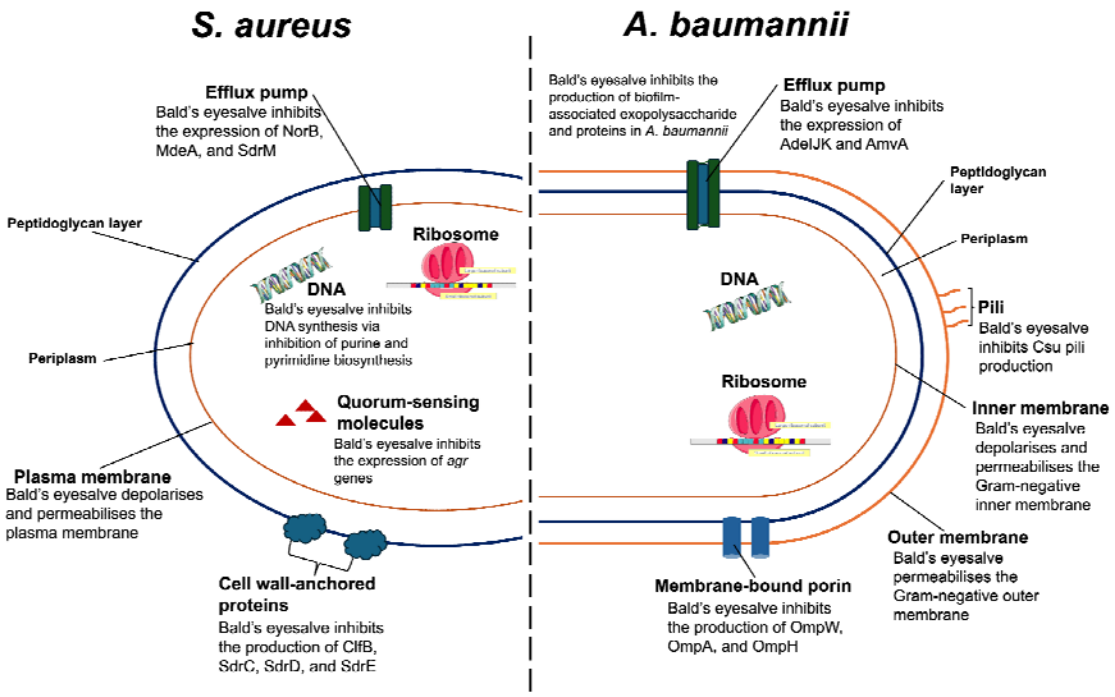

FIG 8. A model for the multifaceted mechanism of action of Bald's eyesalve against *S. aureus* and *A. baumannii*.

Laboratory selection for resistance to Bald's eyesalve led to slower resistance evolution, compared with mainline antibiotics

Resistance evolution is a major challenge in clinical settings, and because various models have predicted that resistance evolution may be harder to achieve for antimicrobials with multiple targets (Li *et al.*, 2025; He *et al.*, 2025), we wanted to check how rapidly or slowly pathogens would evolve resistance to Bald's eyesalve under strong selection for resistance. To achieve this, we carried out a 14-day selection experiment using an evolutionary ramp approach. We initially grew planktonic populations (three populations per bacterial species) of *S. aureus* Newman, *A. baumannii* ATCC 19606, and *P. aeruginosa* PA14 for 24 h in 0.5×MIC of Bald's eyesalve or an example clinically-relevant antibiotic, and then passaged replica aliquots of each population to fresh medium containing either 0.5X or 1×MIC. If a population grew at the higher of the two concentrations, it was passaged to fresh media with 1×MIC and 2×MIC of the treatment; if it failed to grow in the higher concentration, it was

passaged to 0X or 0.5×MIC. In this way, populations that continued to grow were challenged with higher concentrations of treatment, increasing by two-fold each passage after successful growth. The results are shown in (FIG 9) and (Table 2). At the end of day 14, the bacteria were growing in 2-256×MIC of antibiotic, but only 0.5-2×MIC of Bald's eyesalve. Thus, we observed much slower resistance evolution to Bald's eyesalve, suggesting that it is more difficult for bacteria to evolve resistance to this complex cocktail than to single-molecule antibiotics with a narrower range of cellular targets. We also attempted to select for resistant *S. aureus* by serially passaging in a constant sub-inhibitory concentration of ESO for 28 daily transfers. This also failed to generate any resistant mutants (data not shown).

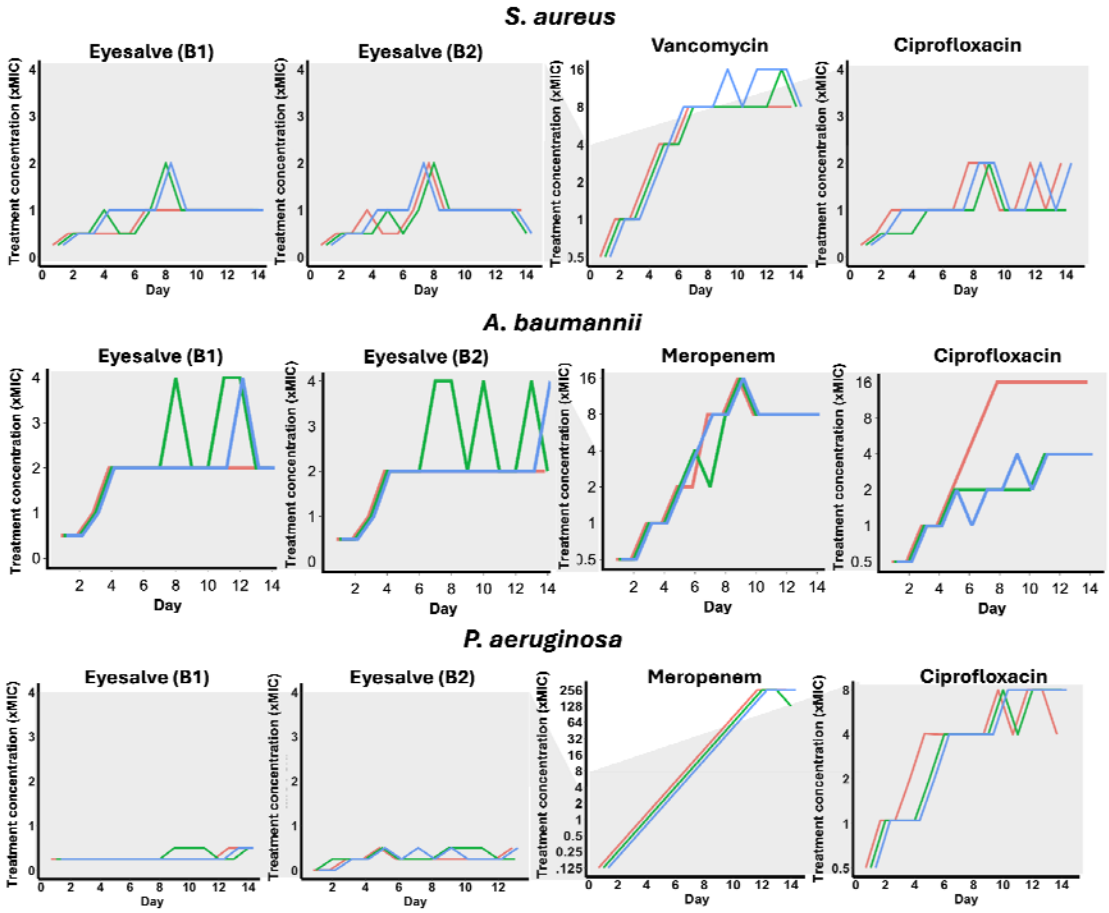

FIG 9. Slower resistance evolution to Bald's eyesalve compared to mainline antibiotics. *S. aureus* Newman, *A. baumannii* ATCC 19606, and *P. aeruginosa* PA14 were subjected to subinhibitory concentrations of Bald's eyesalve or antibiotic and subsequently passaged in different concentrations based on the previous day's highest concentration with growth. This was done for 14 days. The graph's axes show the

highest of two tested concentrations in which cultures grew at each time point, expressed as a multiple of the ancestral MIC.

Table 2. Change in the concentration of Bald's eyesalve in which *S. aureus* Newman, *A. baumannii* ATCC19606, and *P. aeruginosa* PA14 could grow after 14 days of selection in an evolutionary ramp experiment.

Bacteria	Treatment	Fold change in growth concentration at day 14
S. aureus Newman	Vancomycin	8 x MIC
	Ciprofloxacin	2 x MIC
	Eyesalve (batch A)	1 x MIC
	Eyesalve (batch B)	0.5 x MIC
A. baumannii ATCC19606	Meropenem	8 x MIC
	Ciprofloxacin	16 x MIC
	Eyesalve (batch A)	2 x MIC
	Eyesalve (batch B)	4 x MIC
P. aeruginosa PA14	Meropenem	256 x MIC
	Ciprofloxacin	8 x MIC
	Eyesalve (batch A)	0.5 x MIC
	Eyesalve (batch B)	0.5 x MIC

DISCUSSION

The increasing mortality and economic cost associated with AMR have necessitated the need for new antimicrobials (Naghavi *et al.*, 2024; Naylor *et al.*, 2025). It is even more important to have new antimicrobials with multiple modes of action to reduce the risk of resistance. We previously identified a historical remedy called Bald's eyesalve and made a reconstruction of this remedy that had broad-spectrum antibacterial and antibiofilm efficacy against both Gram-positive and Gram-negative pathogens (Harrison *et al.*, 2015; Furner-Pardoe *et al.*,

2020; Anonye *et al.,* 2020). We also showed that this reconstructed historical remedy has great antibacterial activity against *S. aureus*, *S. epidermidis*, *Streptococcus pyogenes*, *Enterococcus cloacae*, *A. baumannii*, and *P. aeruginosa* (Furner-Pardoe *et al.,* 2020). Safety analysis of Bald's eyesalve has so far shown that it has little or no adverse effect in *in vitro* and *in vivo* models (Anonye *et al.,* 2020; Bruce *et al.,* 2022). In this study, we showed that Bald's eyesalve has good antibacterial activity against *S. aureus*, *A. baumannii*, and *P. aeruginosa* in different growth environments. We have also shown that the mechanism of action of this historical remedy is multifaceted.

Using infection-mimicking media for chronic wounds and CF lung infections, we showed that Bald's eyesalve has good antibacterial efficacy against *S. aureus*, *A. baumannii*, and *P. aeruginosa* strains regardless of the growth environment. This is in line with our previous report (Furner-Pardoe *et al.,* 2020). However, we further evidenced that the growth environment has an impact on antimicrobial efficacy, as MIC in the simulated wound fluid was higher than in other media for most of the strains tested. This might be associated with the complex nutrient availability of SWF (Werthén *et al.,* 2010). It is important to emphasise that the bacterial species used in this study are members of the ESKAPE group, and also belongs to the critical (*A. baumannii*) and high (*S. aureus* and *P. aeruginosa*) priority pathogen list for which new drugs are needed, according to the WHO.

In this study, we also showed that Bald's eyesalve has a multifaceted mechanism of action, targeting both cell membrane and intracellular activities. Bald's eyesalve perturbed the membrane potential of both Gram-positive (*S. aureus*) and Gram-negative (*A. baumannii* and *P. aeruginosa*) pathogens. Bacterial membrane potential controls important cellular physiological processes in cells, including membrane transport, motility, ATP synthesis, and cell division (Benarroch and Asally, 2020). This also correlated with the significant expression of membrane-associated transport proteins, including some efflux pump proteins like NorB (*S. aureus*) and AdeT1 (*A. baumannii*). NorB and AdeT1 belong to the major facilitator superfamily (MFS) and resistance nodulation division (RND) classes of efflux pumps, respectively, and confer multidrug resistance on these pathogens (Gaurav *et al.,* 2023). The downregulation of these genes signifies the inhibition of the antimicrobial resistance machineries of these pathogens.

Furthermore, there was inhibition of biofilm-associated genes in both *S. aureus* and *A. baumannii* - most especially, cell surface attachment proteins. The first and essential stage of biofilm formation involves surface or non-surface attachments (Sauer *et al.,* 2022). This attachment stage allows bacterial pathogens to form microcolonies that develop into mature biofilms; hence, an inhibition of this process prevents biofilm formation. The ability of Bald's eyesalve to inhibit biofilm formation by both *S. aureus* and *A. baumannii* was further evidenced in this study. We have also previously shown that Bald's eyesalve has a good killing effect against biofilm-associated *S. aureus* and *A. baumannii* (Furner-Pardoe *et al.,* 2020). Cell surface attachment proteins are also essential for host cell attachment during infections (Smith and Bharat, 2024). In addition to inhibiting attachment, Bald's eyesalve also inhibited other biofilm-associated genes, including those involved in quorum sensing in *S. aureus* and biofilm exopolysaccharide and protein-associated genes in *A. baumannii*. Furthermore, Bald's eyesalve significantly downregulated fatty acid metabolism in *A. baumannii*. Increased fatty acid production has been associated with antibiotic persistence in *A. baumannii* (Vergoz *et al.,* 2024). Hence, the significant downregulation of this process might correlate with increased antibiotic susceptibility in *A. baumannii* to Bald's eyesalve. Also, due to the role of fatty acids in the biosynthesis of phospholipids and lipopolysaccharides in Gram-negative pathogens, inhibition of fatty acid biosynthesis has been suggested as a good target mechanism for new antimicrobials (Cross *et al.,* 2021).

This multifaceted mechanism of action of Bald's eyesalve is likely linked to the combinatorial effect of all its component ingredients. Each of the components (onion, garlic, wine, and bile) of this historical remedy has been reported to have some antibacterial effect. Both garlic (*A. sativum*) and onion (*A. cepa*), the two most popular members of the *Allium* genus and some of the world's oldest crops, are well known for their medicinal benefits (El-Saber *et al.,* 2020; Tesfaye, 2021). These aromatic spices, most especially garlic, have been reported for their bioactivities, including anticancer (Li *et al.,* 2018), antioxidant (Gao and Huang, 2019), antifungal (Li *et al.,* 2016), and antibacterial activities (Magryś *et al.,* 2021; Kshirsagar *et al.,* 2018). The antibacterial activity of garlic has been reported against a broad range of both Gram-positive and Gram-negative pathogens *in vitro* (Magryś *et al.,* 2021; Chen *et al.,* 2018). Some of the common bioactive compounds in garlic and some other *Allium* species include allicin, ajoene, phenols, flavonoids, saponins, triterpenes, steroids, and other organic acids (Tesfaye *et al.,* 2021; Zhang *et al.,* 2020). The most popular and most studied for its antibacterial efficacy, among them, is allicin (Gruhlke *et al.,* 2015; Borlinghaus

et al., 2014). We have previously shown that the antibacterial efficacy of Bald's eyesalve is not just due to the presence of allicin (Furner-Pardoe *et al.,* 2020). Wine, the third component of Bald's eyesalve, is one of the oldest and most popular alcoholic beverages in the world and is mostly produced from the fermentation of grape must or juice (Li *et al.,* 2018). In addition to the popular use of wines for celebrations, they have also been known for centuries for their health benefits due to their variety of bioactive compounds (Mitrovic *et al.,* 2024; Nemzer *et al.,* 2022). Although the optimal antimicrobial activity of wine is majorly due to the combinatorial effect of all its components (pH, alcohol, phenolics, and organic acids) (Boban *et al.,* 2010), the majority of its antimicrobial effect is associated with the different phenolics and organic acids in it (Martínez-Lapuente *et al.,* 2020; Nemzer *et al.,* 2022; Haseeb *et al.,* 2017). Bile, the last component of Bald's eyesalve, have been previously shown to have inhibitory activity against bacterial strains, including *S. aureus* and *P. aeruginosa,* as well as prevent biofilm formation in these strains (Tyagi *et al.,* 2024; Sannasiddappa *et al.,* 2017). The ability of Bald's eyesalve to inhibit *S. aureus* biofilm formation was also evidenced in this study. The antibacterial activity of bile salts has been associated with the disruption of bacterial membranes, leading to the release of intracellular content (Tyagi *et al.,* 2024).

Expectedly, this multifaceted mechanism of action of Bald's eyesalve reduced the risk of resistance evolution against it compared to clinically relevant antibiotics. This is in line with previous studies that reported slow resistance evolution to antimicrobials with multiple targets (Li *et al.,* 2025; He *et al.,* 2025). Additionally, the slower resistance evolution seen with Bald's eyesalve might be associated with its dual effect (depolarisation and permeabilisation) on bacterial membrane (Maharramov *et al.,* 2025). Again, impaired resistance evolution by *S. aureus*, *A. baumannii*, and *P. aeruginosa* against Bald's eyesalve can be linked to the combinatorial effect of its multiple components which target different parts of these bacterial pathogens as shown in this study.

Taking together previous results on Bald's eyesalve's antibacterial and antibiofilm efficacy and the mechanism of action shown in this study, we conclude that this historical remedy has great potential to be used as a foundation for developing an antimicrobial for bacterial infections, especially those resulting from *S. aureus* and *A. baumannii*. Despite the great potential of Bald's eyesalve, we still face current challenges associated with its biofilm eradication activity against *P. aeruginosa* and batch-to-batch variability (Furner-Pardoe *et al.,* 2020). Future studies on Bald's eyesalve should focus on (1) identifying the specific

compounds present that confer antibacterial, antibiofilm and/or antivirulence activity and creating candidate synthetic molecular cocktails for activity testing; and (2) identifying synergists or potentiators that improve the ability of Bald's eyesalve to eradicate *P. aeruginosa* chronic wound biofilm and reduce its batch-to-batch variability.

MATERIALS AND METHODS

Bacterial strains

The bacterial strains used in this study are *S. aureus* Newman, *S. aureus* USA300 LAC, *P. aeruginosa* PA14, *A. baumannii* ATCC 19606, and 5075, *S. aureus* RN6390 P_{xylA}:*gfp*:*luxCDABE* (a growth-dependent reporter), *S. aureus* RN6390 P3:*gfp*:l*uxCDABE* (autoinducing peptide (AIP)-dependent reporter) (Qazi *et al.*, 2001), *P. aeruginosa* NPAO1 (Nottingham PAO1 lab strain) mini-CTX::*luxCDABE* (growth-dependent reporter), and *P. aeruginosa* NPAO1 mini-CTX::*lasB-luxCDABE* (C12-homoserine lactone-dependent reporter). *A. baumannii* 5075 tends to produce small colony variants, and all experiments were started with cultures grown from large colonies from the original culture plate.

Media

The bacteriological media used in this study were phosphate buffered saline (PBS), cation-adjusted Mueller Hinton broth (caMHB) (Sigma-Aldrich, USA), synthetic wound fluid (SWF) (50% v/v foetal bovine serum (Gibco) and 50% v/v peptone water (Sigma-Aldrich, USA) (Werthén *et al.*, 2010), Luria Broth (LB) agar (Sigma-Aldrich, USA), and synthetic cystic fibrosis sputum medium (SCFM, made following the recipe in Palmer *et al.* (2007)).

Bald's eyesalve preparation

Bald's eyesalve was prepared as previously reported (Harrison et al. 2015; Furner-Pardoe *et al.*, 2020). Briefly, equal volumes of onion and garlic sourced locally were chopped separately into pieces with a sterile knife and then pounded together with a sterile mortar and pestle for 2 min. Equal amounts of wine (Pennard Organic, Somerset, UK) and oxgall (Sigma Aldrich, USA) were then added, and the mixture was placed in a sterile 250 ml Duran bottle covered with aluminium foil. The bottle was placed in the fridge (at 4°C) for 9 days. After 9 days, the lumps in the bottle were strained and the liquid transferred into sterile 50 ml Falcon tubes. The tubes were centrifuged at 3000 rpm for 5 minutes, after which the liquid was filtered into 2 ml Eppendorf tubes with a sterile syringe and a 5 µm filter. Samples were stored in -20°C for further analysis.

Minimum inhibitory concentration assay

The broth microdilution method was used to determine the minimum inhibitory concentration of the antimicrobials as recommended by the European Committee on Antimicrobial Susceptibility Testing (EUCAST). Briefly, the bacterial strain of interest was streaked on LB agar and incubated at 37°C for 18-24 h to produce distinct colonies. Twice the maximum concentration of the antibiotics to be used was prepared in the medium of interest (caMHB, SWF, and SCFM) and dispensed (100 µl) in the first column of a Corning Costar CLS9018 (Corning Inc., US) 96-well plate. Fifty microlitres of the medium were then dispensed into each of the other wells, after which a two-fold serial dilution was carried out. A bacterial suspension in the medium was prepared by touching 3-4 distinct colonies with a sterile cotton swab and dispersing them in PBS. This was then standardised to a 0.5 MacFarland standard with a spectrophotometer (OD600nm = 0.08-0.10). The standardised bacterial suspension (50 µl) was then inoculated into triplicate wells of each concentration except for the sterile control well (without antimicrobials and bacteria). Growth control wells (with only bacteria) were also set up. The 96-well plates were sealed with Parafilm™ and incubated at 37°C for 18-24 h. The lowest concentration well with no observable growth is taken as the MIC. After incubation, an inoculum of 10 µl was spotted out onto LB agar from each of the wells to determine the minimum bactericidal concentration (MBC). The LB agar plates were incubated at 37°C for 18-24 h. The concentration with no growth on the LB agar was taken as the MBC. Uninoculated media (without antibiotics) were used as a negative control, while bacterial suspension without antibiotics was used as a positive control.

DiSC3(5) kinetics assay for cell membrane disruption

A DiSC3(5) (3,3'-Dipropylthiadicarbocyanine iodide) assay was performed as previously described by Buttress et al. (2022) with a little modification. Briefly, bacterial culture growing at the exponential phase in LB was diluted to 0.5 OD_{600} with PBS containing 0.5 mg/ml bovine serum albumin (BSA) (Sigma-Aldrich, UK) and 2 µM glucose. The addition of BSA was to prevent the binding of DiSC3(5) reagent to the microtitre plate. For *S. aureus*, cells were washed in PBS containing 0.5 mg/ml bovine serum albumin (BSA) (Sigma-Aldrich, UK) and 2 µM glucose twice and then resuspended. After resuspension, the tube containing washed cells was incubated for 15 min. For the Gram-negative bacterial strains (*A. baumannii* and *P. aeruginosa*), diluted bacteria were incubated directly for 15 min, skipping the washing step to avoid disrupting the outer membrane. Bacteria were then transferred into

a black polystyrene 96-well plate (Corning Inc., US) and autofluorescence measured (excitation wavelength = 610±10, emission wavelength = 660±10) for 5 min in Tecan SPARK 10 M (Tecan, Switzerland) plate reader, after which an equal volume of 1 µM DiSC3(5) reagent (Invitrogen) in 1% DMSO was added to give a final DiSC3(5) concentration of 0.5 µM and fluorescence measured for another 5 minutes. Treatments were then added, and the fluorescence was monitored for 1 h. For experiments with *A. baumannii* and *P. aeruginosa*, bacterial culture was pre-incubated with 30 µg/ml polymixin B nanopeptide for 15 minutes before transferring to the 96-well plate as recommended by Buttress *et al.* (2022). This permeabilises the outer membrane to allow the treatments to access the plasma membrane.

Cytological profiling with FM4-64 dye

Overnight cultures of bacteria were grown to mid-exponential phase and diluted to 0.1-0.2 OD600 in caMHB. The diluted cultures were then treated with media, 2×MIC of Bald's eyesalve, and 2×MIC of cocktail (SWF) for 1 h, 2 h, and 3 h. Cells were then washed by centrifuging at 10,000 rpm for 5 min and resuspended in PBS. FM4-64 was then added to a final concentration of 2.5 µg/ml and incubated for 15-20 min. The stain was then washed, and cells were fixed with formaldehyde. The images were taken with a Nikon Eclipse-Ti wide-field fluorescence microscope at oil immersion magnification.

Propidium iodide assay

A membrane permeabilisation assay was carried out as previously described by Boix-Lemonche (2020), with modifications. First, bacteria at mid-log phase of growth in LB were diluted to an 0.1 OD_{600} with PBS containing 2 µM glucose, transferred (50 µl) into a black 96-well flat bottom plate CLS3596 (Corning Inc., US) and autofluorescence (excitation wavelength = 530±20, emission wavelength = 620±10) was measured for 5 min in Tecan SPARK 10 M (Tecan, Switzerland) plate reader. Propidium iodide (50 µl) (Invitrogen) was added to the wells at a final concentration of 50 µg/ml, followed by fluorescence measurement for another 5 min. Treatments were then added, after which fluorescence was measured for 1 h.

Scanning electron microscopy

Overnight bacterial culture was resuspended in caMHB to 0.1 OD_{600} and incubated on a shaker at 37°C until it reached mid-exponential phase (10^6 to 10^7 CFU/ml). Cultures were

then diluted (equal volume) with treatment (Bald's eyesalve, or caMHB (control)) and incubated for 2 h. Bacterial cells were then centrifuged at 10000 rpm for 1 min, followed by 3 washes of PBS. Twelve (12) millimetre coverslips (VWR, US) were then incubated with 50 µl of poly-lysine (Sigma-Aldrich, US) for 15 min, after which the poly-lysine was removed and the coverslips left to dry. Bacterial cell pellets were resuspended in 400 µl of PBS, after which 50 µl of this was added to each cover slip (in a 24-well plate) and incubated for 30 min at 37°C. Excess (unbound) bacterial suspension was then discarded, and the bound cells were fixed with 2.5% glutaraldehyde solution in PBS overnight. After fixing, excess glyceraldehyde was removed, and the coverslips were washed 3 times with PBS. The coverslips were transferred into clean wells and dehydrated using ethanol gradient (20%, 50%, 70%, 90%, 100%, and 100%) for 10 min in each ethanol concentration. The coverslips were then transferred into new wells and incubated with 0.5 ml of hexamethyldisilazane (HDMS) for 30 min. The coverslips were then moved again into new wells, the HDMS discarded, and the slips were left to dry in a laminar flow cabinet for 30 min. Coverslips were then added to copper tapes placed on SEM sample holders, and the samples were sputtered with carbon. The images were taken with the Zeiss Gemini Scanning Electron Microscope at the Warwick Electron Microscope Research Technology Platform.

Negative staining and transmission electron microscopy

S. aureus Newman was grown in SWF for 6h to allow cells to reach the exponential phase in a 96-well plate. In the wells, 50 µl of treatment (water, nisin – 150 µg/ml, vancomycin – 100 µg/ml, and 100% Bald's eyesalve) was added to 100 µl of bacterial cells and incubated for 4 h at 37 °C. Cells (100 µl) were centrifuged at 3,200 g for 10 min, washed in PBS, and resuspended in 100 µl of PBS. Cells were then fixed in 4% PFA for 15 min and washed in PBS. ELMO glow discharge (Courdouan Technologies) was used to glow-discharge the carbon film for 1 min, after which 10 µl of the sample was loaded on the carbon film and excess liquid removed with filter paper. Ten microlitres of uranium acetate was added to the sample, left for 2 min, after which the samples were imaged with a JEOL 2100 transmission electron microscope.

RNA sample preparation and sequence analysis

Overnight cultures of bacteria were diluted to 0.1 OD_{600} in caMHB, grown to mid-exponential phase, and diluted to 0.4 OD_{600}. Equal volume (500 µl) of either Bald's eyesalve

or media (control) was added to culture at 2×MIC to make up a final volume of 1 ml. The treated cultures (*A. baumannii* ATCC 19606 and *S. aureus* Newman) were incubated for 2 h, after which the media and treatment were washed off by centrifuging at 10,000 rpm for 10 min. Cell pellets were then resuspended in PBS, centrifuged at 10,000 rpm for 10 min, snap frozen, and sent for RNA extraction and sequencing by Genewiz. Quality of the raw fastq files was checked with fastqc (Leggett *et al.,* 2013), after which trimommatic (Bolger *et al.,* 2014) was used to remove Illumina adapter sequences from the reads. Alignment was done with Bowtie2 (Langmead and Salzberg, 2012). For *S. aureus*, all reads were aligned to *S. aureus* Newman whole genome sequence (accession number - NC009641.1, assembly - GCF_000010465.1), while *A. baumannii* reads were aligned to *A. baumannii* ATCC 19606 whole genome sequence (accession number - NZ_CP046654.1, assembly - GCF_009759685.1). The aligned sam files were converted to bam format using samtools (Li *et al.,* 2009), after which featureCounts (Liao *et al.,* 2014) was used to obtain read counts. DESeq2 (Love *et al.,* 2014) in R v4.3.3 (R Core Team, 2023) was then used to determine differentially expressed genes, while Gene Ontology (GO) analysis was performed with FUNAGEpro v3 (Anne *et al.,* 2023).

Quorum-sensing assay

Overnight cultures of *S. aureus* RN6390 P_{xylA}:*gfp*:*luxCDABE* (a growth-dependent reporter), *S. aureus* RN6390 P3:*gfp*:l*uxCDABE* (autoinducing peptide (AIP)-dependent reporter) (Qazi *et al.,* 2001), *P. aeruginosa* NPAO1 (Nottingham PAO1 lab strain) mini-CTX::*luxCDABE* (growth-dependent reporter), and *P. aeruginosa* NPAO1 mini-CTX::*lasB-luxCDABE* (C12-homoserine lactone-dependent reporter) (Righetti, 2011) on LB were diluted to 0.1-0.2 OD_{600} and allowed to grow to mid-exponential phase in SWF, after which cells were diluted to 0.08-0.1 OD_{600}. Two hundred microlitres (200 µl) of the diluted cultures were added to wells of a black 96-well flat-bottom microtitre plate CLS3596 (Corning Inc., US). After which 100 µl of treatment (sterile distilled water (control), 1/10 Bald's eyesalve (10%), 1/100 Bald's eyesalve (1%), 1/1000 Bald's eyesalve (0.1%)) was added to the wells in triplicate. The plate was incubated at 37ºC for 20 h with periodic shaking in a Tecan SPARK 10 M (Tecan, Switzerland) plate reader, and the optical density (OD_{600}) and luminescence of the wells (relative luminescence units, RLU) were taken every 15 minutes. Reporter gene expression was expressed as RLU/ OD_{600}.

Long-term evolution experiment

A long-term evolution experiment was carried out to determine the resistance evolution pattern of *S. aureus* and *P. aeruginosa* to both Bald's eyesalve and its derived cocktail as previously described (Jorth *et al.*, 2017) with modifications. Briefly, the MICs of the treatments (Bald's eyesalve, SWF, meropenem (for *P. aeruginosa*), vancomycin (for *S. aureus*), and ciprofloxacin (both)) against the bacterial strains (*S. aureus* and *P. aeruginosa*), in each of the media (caMHB, SWF) were first determined as previously described. Two microlitres (2 µl) of bacterial inoculum at approximately 10^5 CFU was taken from the 0.5×MIC well and added to a new 96-well plate CL3596 (Corning Inc., US) containing 198 µl of media with 0.5×MIC and 1×MIC of the treatments to make a final volume of 200 µl in each well. There were 3 wells per treatment. The plates were sealed with Parafilm™ and incubated at 37°C for 20-24 h without shaking. For each treatment, bacteria from the well containing the highest treatment concentration with visible growth were selected for passage to fresh medium. Two microlitres (2 µl) of culture from these wells were inoculated into duplicate wells of fresh medium (198 µl) containing 1× and 2× the concentration of treatment present in the originating well. If no growth was seen in the presence of the lower concentration, the concentrations were adjusted to 0.5× the lowest concentration of the previous day. This process was repeated for 14 days. Clones were stored in 25% glycerol in LB at -80°C.

AUTHOR CONTRIBUTIONS

Author contributions following CRedit Taxonomy:

Conceptualisation: FH, OO, CC.

Investigation: OO, JF-P, BA, JR, NR, FH.

Formal analysis: OO, JF-P.

Methodology (methods development): SH, NEH, RGM.

Methodology (pilot investigation): AG, SS.

Supervision: FH, CC, SH, SPD, OO.

Writing – original draft: OO, FH.

Writing – review & editing: all authors.

ACKNOWLEDGMENTS

We thank Christina Lee and Aled Roberts for all of the work and discussion that led to the foundation of the Ancientbiotics team and, ultimately, the present research. We thank Ian Hands-Portman and the Warwick Microscopy Bio-Analytical Shared Resource Laboratory

for assistance with TEM; The Warwick Electron Microscope Research Technology Platform for use of SEM; Alan Cockayne, Kim Hardie and Kendra Rumbaugh for supplying bacterial strains; and Cerith Harries and Charlotte Curtis of the Warwick School of Life Science Media Preparation Service for supplying media and plates. This work benefited greatly from discussion and feedback on JFP and OO's PhD theses from Antonia Sagona, Cassandra Quave, Henrik Strahl, Christopher Rodrigues and Stephen Parnell. A large number of lab members and students past and present contributed to the prior research that led to the present work, and we thank them all - especially Jason Millington and Thorulf Vargsen for contributing to a pilot resistance evolution experiment. We also gratefully acknowledge the support of the University of Warwick Institute of Advanced Studies (IAS) through an Early Career Fellowship awarded to OQO during the writing up of this manuscript.

ETHICS APPROVAL

No ethical approval was required for this study.

FUNDING

This work was funded by the Biotechnology and Biological Sciences Research Council (Midlands Integrative Biosciences Training Partnership studentship awarded to OQO, [grant number BB/T00746X/1]); the Medical Research Council (Doctoral Training Programme in Interdisciplinary Biomedical Research studentships granted to JFP, NR, RGM & JR [grant numbers MR/N014294/1 and MR/W007053/1]; Diabetes UK (project grant awarded to FH, [grant number 17_0005690]); the University of Warwick (MBio projects for AG & SS); and the University of Nottingham (UNICAS sandpit award to SPD & FH).

CONFLICTS OF INTEREST

The authors declare no conflict of interest.

REFERENCES

Naghavi, M., Vollset, S. E., Ikuta, K. S., Swetschinski, L. R., Gray, A. P., Wool, E. E., Robles Aguilar, G., Mestrovic, T., Smith, G., Han, C., Hsu, R. L., Chalek, J., Araki, D. T., Chung, E., Raggi, C., Gershberg Hayoon, A., Davis Weaver, N., Lindstedt, P. A., Smith, A. E., . . . Murray, C. J. L. (2024). Global burden of bacterial antimicrobial

resistance 1990–2021: a systematic analysis with forecasts to 2050. *The Lancet*, *404*(10459), 1199-1226. https://doi.org/10.1016/s0140-6736(24)01867-1

Naylor, N. R., Hasso-Agopsowicz, M., Kim, C., Ma, Y., Frost, I., Abbas, K., Aguilar, G., Fuller, N., Robotham, J. V., & Jit, M. (2025). The global economic burden of antibiotic-resistant infections and the potential impact of bacterial vaccines: a modelling study. *BMJ Global Health*, *10*(6), e016249. https://doi.org/10.1136/bmjgh-2024-016249

Ahmed, S. K., Hussein, S., Qurbani, K., Ibrahim, R. H., Fareeq, A., Mahmood, K. A., & Mohamed, M. G. (2024). Antimicrobial resistance: Impacts, challenges, and future prospects. *Journal of Medicine, Surgery, and Public Health*, *2*, 100081. https://doi.org/https://doi.org/10.1016/j.glmedi.2024.100081

Prasad, N. K., Seiple, I. B., Cirz, R. T., & Rosenberg, O. S. (2022). Leaks in the Pipeline: a Failure Analysis of Gram-Negative Antibiotic Development from 2010 to 2020. *Antimicrobial Agents and Chemotherapy*, *66*(5). https://doi.org/10.1128/aac.00054-22

Kavanagh, K. (2025). The rise of 'nightmare bacteria': antimicrobial resistance in five charts. *Nature*, *646*(8085), 526-527. https://doi.org/10.1038/d41586-025-03218-x

Woods, R. J., & Read, A. F. (2023). Combination antimicrobial therapy to manage resistance. *Evolution, Medicine, and Public Health*, *11*(1), 185-186. https://doi.org/10.1093/emph/eoad005

Si, Z., Pethe, K., & Chan-Park, M. B. (2023). Chemical Basis of Combination Therapy to Combat Antibiotic Resistance. *JACS Au*, *3*(2), 276-292. https://doi.org/10.1021/jacsau.2c00532

Yahav, D., Giske, C. G., Grāmatniece, A., Abodakpi, H., Tam, V. H., & Leibovici, L. (2020). New β-Lactam–β-Lactamase Inhibitor Combinations. *Clinical Microbiology Reviews*, *34*(1), 10.1128/cmr.00115-00120. https://doi.org/doi:10.1128/cmr.00115-20

Ogwu, M. C., & Izah, S. C. (2025). Honey as a Natural Antimicrobial. *Antibiotics*, *14*(3), 255. https://doi.org/10.3390/antibiotics14030255

Eteraf-Oskouei, T., & Najafi, M. (2013). Traditional and modern uses of natural honey in human diseases: a review. *Iran J Basic Med Sci*, *16*(6), 731-742.

Sharaf El-Din, M. G., Farrag, A. F. S., Wu, L., Huang, Y., & Wang, K. (2025). Health benefits of honey: A critical review on the homology of medicine and food in traditional and modern contexts. *Journal of Traditional Chinese Medical Sciences*, *12*(2), 147-164. https://doi.org/https://doi.org/10.1016/j.jtcms.2025.03.015

Muhs, A., Lyles, J. T., Parlet, C. P., Nelson, K., Kavanaugh, J. S., Horswill, A. R., & Quave, C. L. (2017). Virulence Inhibitors from Brazilian Peppertree Block Quorum Sensing and Abate Dermonecrosis in Skin Infection Models. *Scientific Reports*, *7*(1), 42275. https://doi.org/10.1038/srep42275

Caesar, L. K., & Cech, N. B. (2019). Synergy and antagonism in natural product extracts: when 1 + 1 does not equal 2. *Natural Product Reports*, *36*(6), 869-888. https://doi.org/10.1039/c9np00011a

Tu, Y. (2011). The discovery of artemisinin (qinghaosu) and gifts from Chinese medicine. *Nature Medicine*, *17*(10), 1217-1220. https://doi.org/10.1038/nm.2471

Gruessner, B. M., Cornet-Vernet, L., Desrosiers, M. R., Lutgen, P., Towler, M. J., & Weathers, P. J. (2019). It is not just artemisinin: Artemisia sp. for treating diseases including malaria and schistosomiasis. *Phytochemistry Reviews*, *18*(6), 1509-1527. https://doi.org/10.1007/s11101-019-09645-9

Connelly, E., Lee, C., Furner-Pardoe, J., Del Genio, C. I., & Harrison, F. (2022). A case study of the Ancientbiotics collaboration. *Patterns*, *3*(12), 100632. https://doi.org/10.1016/j.patter.2022.100632

Harrison, F., Roberts, A. E. L., Gabrilska, R., Rumbaugh, K. P., Lee, C., & Diggle, S. P. (2015). A 1,000-Year-Old Antimicrobial Remedy with Antistaphylococcal Activity. *mBio*, *6*(4), 10.1128/mbio.01129-01115. https://doi.org/doi:10.1128/mbio.01129-15

Furner-Pardoe, J., Anonye, B. O., Cain, R., Moat, J., Ortori, C. A., Lee, C., Barrett, D. A., Corre, C., & Harrison, F. (2020). Anti-biofilm efficacy of a medieval treatment for bacterial infection requires the combination of multiple ingredients. *Sci Rep*, *10*(1), 12687. https://doi.org/10.1038/s41598-020-69273-8

Anonye, B. O., Nweke, V., Furner-Pardoe, J., Gabrilska, R., Rafiq, A., Ukachukwu, F., Bruce, J., Lee, C., Unnikrishnan, M., Rumbaugh, K. P., Snyder, L. A. S., & Harrison, F. (2020). The safety profile of Bald's eyesalve for the treatment of bacterial infections. *Scientific Reports*, *10*(1). https://doi.org/10.1038/s41598-020-74242-2

Bruce, J., Oyedemi, B., Parsons, N., & Harrison, F. (2022). Phase 1 safety trial of a natural product cocktail with antibacterial activity in human volunteers. *Scientific Reports*, *12*(1), 19656. https://doi.org/10.1038/s41598-022-22700-4

Murray, C. J., Ikuta, K. S., Sharara, F., Swetschinski, L., Robles Aguilar, G., Gray, A., Han, C., Bisignano, C., Rao, P., Wool, E., Johnson, S. C., Browne, A. J., Chipeta, M. G., Fell, F., Hackett, S., Haines-Woodhouse, G., Kashef Hamadani, B. H., Kumaran, E. A. P., McManigal, B., . . . Naghavi, M. (2022). Global burden of bacterial

antimicrobial resistance in 2019: a systematic analysis. *The Lancet*, *399*(10325), 629-655. https://doi.org/10.1016/s0140-6736(21)02724-0

Werthén, M., Henriksson, L., Jensen, P., Sternberg, C., Givskov, M., & Bjarnsholt, T. (2010). An in vitro model of bacterial infections in wounds and other soft tissues. *Apmis*, *118*(2), 156-164. https://doi.org/10.1111/j.1600-0463.2009.02580.x

Palmer, K. L., Aye, L. M., & Whiteley, M. (2007). Nutritional Cues Control Pseudomonas aeruginosa Multicellular Behavior in Cystic Fibrosis Sputum. *Journal of Bacteriology*, *189*(22), 8079-8087. https://doi.org/doi:10.1128/jb.01138-07

Ersoy, S. C., Heithoff, D. M., Barnes, L., Tripp, G. K., House, J. K., Marth, J. D., Smith, J. W., & Mahan, M. J. (2017). Correcting a Fundamental Flaw in the Paradigm for Antimicrobial Susceptibility Testing. *EBioMedicine*, *20*, 173-181. https://doi.org/10.1016/j.ebiom.2017.05.026

Sweeney, E., Sabnis, A., Edwards, A. M., & Harrison, F. (2020). Effect of host-mimicking medium and biofilm growth on the ability of colistin to kill Pseudomonas aeruginosa. *Microbiology*, *166*(12), 1171-1180. https://doi.org/10.1099/mic.0.000995

Garidel, P., Hildebrand, A., Knauf, K., & Blume, A. (2007). Membranolytic Activity of Bile Salts: Influence of Biological Membrane Properties and Composition. *Molecules*, *12*(10), 2292-2326. https://doi.org/10.3390/12102292

Gruhlke, M. C., Hemmis, B., Noll, U., Wagner, R., Lühring, H., & Slusarenko, A. J. (2015). The defense substance allicin from garlic permeabilizes membranes of Beta vulgaris, Rhoeo discolor, Chara corallina and artificial lipid bilayers. *Biochim Biophys Acta*, *1850*(4), 602-611. https://doi.org/10.1016/j.bbagen.2014.11.020

Loison, P., Gervais, P., Perrier-Cornet, J.-M., & Kuimova, M. K. (2016). Effect of ethanol perturbation on viscosity and permeability of an inner membrane in Bacillus subtilis spores. *Biochimica et Biophysica Acta (BBA) - Biomembranes*, *1858*(9), 2060-2069. https://doi.org/https://doi.org/10.1016/j.bbamem.2016.06.003

Ji, Q.-Y., Wang, W., Yan, H., Qu, H., Liu, Y., Qian, Y., & Gu, R. (2023). The Effect of Different Organic Acids and Their Combination on the Cell Barrier and Biofilm of Escherichia coli. *Foods*, *12*(16), 3011. https://doi.org/10.3390/foods12163011

Buttress, J. A., Halte, M., Te Winkel, J. D., Erhardt, M., Popp, P. F., & Strahl, H. (2022). A guide for membrane potential measurements in Gram-negative bacteria using voltage-sensitive dyes. *Microbiology*, *168*(9). https://doi.org/10.1099/mic.0.001227

Szalai, B., & Veres, D. V. (2023). Application of perturbation gene expression profiles in drug discovery—From mechanism of action to quantitative modelling. *Frontiers in Systems Biology*, *3*. https://doi.org/10.3389/fsysb.2023.1126044

Hudson, M. A., & Lockless, S. W. (2022). Elucidating the Mechanisms of Action of Antimicrobial Agents. *mBio*, *13*(3). https://doi.org/10.1128/mbio.02240-21

Whittle, E. E., Orababa, O., Osgerby, A., Siasat, P., Element, S. J., Blair, J. M. A., & Overton, T. W. (2024). Efflux pumps mediate changes to fundamental bacterial physiology via membrane potential. *mBio*, *15*(10), e02370-02324. https://doi.org/doi:10.1128/mbio.02370-24

Zhu, Z., Hu, Z., Li, S., Fang, R., Ono, H. K., & Hu, D.-L. (2023). Molecular Characteristics and Pathogenicity of Staphylococcus aureus Exotoxins. *International Journal of Molecular Sciences*, *25*(1), 395. https://doi.org/10.3390/ijms25010395

Wang, M., Li, X., Cavallo, F. M., Yedavally, H., Piersma, S., Raineri, E. J. M., Vera Murguia, E., Kuipers, J., Zhang, Z., van Dijl, J. M., & Buist, G. (2024). Functional profiling of CHAP domain-containing peptidoglycan hydrolases of Staphylococcus aureus USA300 uncovers potential targets for anti-staphylococcal therapies. *International Journal of Medical Microbiology*, *316*, 151632. https://doi.org/https://doi.org/10.1016/j.ijmm.2024.151632

Borlinghaus, J., Albrecht, F., Gruhlke, M. C., Nwachukwu, I. D., & Slusarenko, A. J. (2014). Allicin: chemistry and biological properties. *Molecules*, *19*(8), 12591-12618. https://doi.org/10.3390/molecules190812591

Goncheva, M. I., Chin, D., & Heinrichs, D. E. (2022). Nucleotide biosynthesis: the base of bacterial pathogenesis. *Trends in Microbiology*, *30*(8), 793-804. https://doi.org/10.1016/j.tim.2021.12.007

Stevens, C. E., Deventer, A. T., & Hobbs, J. K. (2025). The impact of bacterial purine metabolism on antibiotic efficacy. *npj Antimicrobials and Resistance*, *3*(1). https://doi.org/10.1038/s44259-025-00139-7

Liu, Y., Su, S., Yu, M., Zhai, D., Hou, Y., Zhao, H., Ma, X., Jia, M., Xue, X., & Li, M. (2022). Pyrancoumarin derivative LP4C targeting of pyrimidine de novo synthesis pathway inhibits MRSA biofilm and virulence. *Frontiers in Pharmacology*, *13*. https://doi.org/10.3389/fphar.2022.959736

Vergoz, D., Schaumann, A., Schmitz, I., Afonso, C., Dé, E., Loutelier-Bourhis, C., & Alexandre, S. (2024). Lipidome of Acinetobacter baumannii antibiotic persister cells.

Biochimica et Biophysica Acta (BBA) - Molecular and Cell Biology of Lipids, *1869*(7), 159539. https://doi.org/https://doi.org/10.1016/j.bbalip.2024.159539

Li, H., Kang, W.-T., Zheng, Y., He, Y., Zhong, R., Fang, S., Wen, W., Liu, S., & Lin, S. (2025). Development of xanthone derivatives as effective broad-spectrum antimicrobials: Disrupting cell wall and inhibiting DNA synthesis. *Science Advances*, *11*(10). https://doi.org/10.1126/sciadv.adt4723

He, W., Huan, X., Li, Y., Deng, Q., Chen, T., Xiao, W., Chen, Y., Ma, L., Liu, N., Shang, Z., & Wang, Z. (2025). A broad-spectrum antibiotic targets multiple-drug-resistant bacteria with dual binding targets and no detectable resistance. *Nature Communications*, *16*(1). https://doi.org/10.1038/s41467-025-62407-4

El-Saber Batiha, G., Magdy Beshbishy, A., G. Wasef, L., Elewa, Y. H. A., A. Al-Sagan, A., Abd El-Hack, M. E., Taha, A. E., M. Abd-Elhakim, Y., & Prasad Devkota, H. (2020). Chemical Constituents and Pharmacological Activities of Garlic (Allium sativum L.): A Review. *Nutrients*, *12*(3), 872. https://doi.org/10.3390/nu12030872

Tesfaye, A. (2021). Revealing the Therapeutic Uses of Garlic (Allium sativum) and Its Potential for Drug Discovery. *The Scientific World Journal*, *2021*, 1-7. https://doi.org/10.1155/2021/8817288

Li, W.-R., Shi, Q.-S., Dai, H.-Q., Liang, Q., Xie, X.-B., Huang, X.-M., Zhao, G.-Z., & Zhang, L.-X. (2016). Antifungal activity, kinetics and molecular mechanism of action of garlic oil against Candida albicans. *Scientific Reports*, *6*(1), 22805. https://doi.org/10.1038/srep22805

Gao, H., & Huang, G. (2019). Preparation and antioxidant activity of carboxymethylated garlic polysaccharide. *International Journal of Biological Macromolecules*, *121*, 650-654. https://doi.org/https://doi.org/10.1016/j.ijbiomac.2018.10.094

Li, Z., Le, W., & Cui, Z. (2018). A novel therapeutic anticancer property of raw garlic extract via injection but not ingestion. *Cell Death Discovery*, *4*(1). https://doi.org/10.1038/s41420-018-0122-x

Magryś, A., Olender, A., & Tchórzewska, D. (2021). Antibacterial properties of Allium sativum L. against the most emerging multidrug-resistant bacteria and its synergy with antibiotics. *Archives of Microbiology*, *203*(5), 2257-2268. https://doi.org/10.1007/s00203-021-02248-z

Kshirsagar, M. M., Dodamani, A. S., Karibasappa, G. N., Vishwakarma, P. K., Vathar, J. B., Sonawane, K. R., Jadhav, H. C., & Khobragade, V. R. (2018). Antibacterial activity

of garlic extract on cariogenic bacteria: An in vitro study. *Ayu*, *39*(3), 165-168. https://doi.org/10.4103/ayu.AYU_193_16

Chen, C., Liu, C.-H., Cai, J., Zhang, W., Qi, W.-L., Wang, Z., Liu, Z.-B., & Yang, Y. (2018). Broad-spectrum antimicrobial activity, chemical composition and mechanism of action of garlic (Allium sativum) extracts. *Food Control*, *86*, 117-125. https://doi.org/https://doi.org/10.1016/j.foodcont.2017.11.015

Zhang, Y., Liu, X., Ruan, J., Zhuang, X., Zhang, X., & Li, Z. (2020). Phytochemicals of garlic: Promising candidates for cancer therapy. *Biomedicine & Pharmacotherapy*, *123*, 109730. https://doi.org/https://doi.org/10.1016/j.biopha.2019.109730

Li, H., Wang, H., Li, H., Goodman, S., van der Lee, P., Xu, Z., Fortunato, A., & Yang, P. (2018). The worlds of wine: Old, new and ancient. *Wine Economics and Policy*, *7*(2), 178-182. https://doi.org/https://doi.org/10.1016/j.wep.2018.10.002

Mitrović, D., Sredović Ignjatović, I., Kozarski, M., & Popović Đorđević, J. (2024). Wine is more than just a beverage: Chemical diversity, health benefits, and immunomodulating potential of wine polyphenols. *Food Safety and Health*, *2*(2), 196-212. https://doi.org/10.1002/fsh3.12036

Nemzer, B., Kalita, D., Yashin, A. Y., & Yashin, Y. I. (2022). Chemical Composition and Polyphenolic Compounds of Red Wines: Their Antioxidant Activities and Effects on Human Health—A Review. *Beverages*, *8*(1), 1. https://www.mdpi.com/2306-5710/8/1/1

Boban, N., Tonkic, M., Budimir, D., Modun, D., Sutlovic, D., Punda-Polic, V., & Boban, M. (2010). Antimicrobial effects of wine: separating the role of polyphenols, pH, ethanol, and other wine components. *J Food Sci*, *75*(5), M322-326. https://doi.org/10.1111/j.1750-3841.2010.01622.x

Martínez-Lapuente, L., Guadalupe, Z., & Ayestarán, B. (2020). Properties of Wine Polysaccharides. In. IntechOpen. https://doi.org/10.5772/intechopen.85629

Haseeb, S., Alexander, B., & Baranchuk, A. (2017). Wine and Cardiovascular Health. *Circulation*, *136*(15), 1434-1448. https://doi.org/10.1161/circulationaha.117.030387

Tyagi, A., Kumar, V., Joshi, N., & Dhingra, H. K. (2024). Exploring the Antibacterial Potential of Bile Salts: Inhibition of Biofilm Formation and Cell Growth in Pseudomonas aeruginosa and Staphylococcus aureus. *Microbiology Research*, *15*(3), 1269-1279. https://doi.org/10.3390/microbiolres15030085

Sannasiddappa, T. H., Lund, P. A., & Clarke, S. R. (2017). In Vitro Antibacterial Activity of Unconjugated and Conjugated Bile Salts on Staphylococcus aureus. *Frontiers in Microbiology*, *8*. https://doi.org/10.3389/fmicb.2017.01581

Benarroch, J. M., & Asally, M. (2020). The Microbiologist's Guide to Membrane Potential Dynamics. *Trends Microbiol*, *28*(4), 304-314. https://doi.org/10.1016/j.tim.2019.12.008

Gaurav, A., Bakht, P., Saini, M., Pandey, S., & Pathania, R. (2023). Role of bacterial efflux pumps in antibiotic resistance, virulence, and strategies to discover novel efflux pump inhibitors. *Microbiology (Reading)*, *169*(5). https://doi.org/10.1099/mic.0.001333

Sauer, K., Stoodley, P., Goeres, D. M., Hall-Stoodley, L., Burmølle, M., Stewart, P. S., & Bjarnsholt, T. (2022). The biofilm life cycle: expanding the conceptual model of biofilm formation. *Nature Reviews Microbiology*, *20*(10), 608-620. https://doi.org/10.1038/s41579-022-00767-0

Smith, O. E. R., & Bharat, T. A. M. (2024). Architectural dissection of adhesive bacterial cell surface appendages from a “molecular machines” viewpoint. *Journal of Bacteriology*, *206*(12). https://doi.org/10.1128/jb.00290-24

Boix-Lemonche, G., Lekka, M., & Skerlavaj, B. (2020). A Rapid Fluorescence-Based Microplate Assay to Investigate the Interaction of Membrane Active Antimicrobial Peptides with Whole Gram-Positive Bacteria. *Antibiotics (Basel)*, *9*(2). https://doi.org/10.3390/antibiotics9020092

Jorth, P., McLean, K., Ratjen, A., Secor, P. R., Bautista, G. E., Ravishankar, S., Rezayat, A., Garudathri, J., Harrison, J. J., Harwood, R. A., Penewit, K., Waalkes, A., Singh, P. K., & Salipante, S. J. (2017). Evolved Aztreonam Resistance Is Multifactorial and Can Produce Hypervirulence in Pseudomonas aeruginosa. *mBio*, *8*(5). https://doi.org/10.1128/mbio.00517-17

Anne, Kuipers, O. P., & Kok, J. (2022). FUNAGE-Pro: comprehensive web server for gene set enrichment analysis of prokaryotes. *Nucleic Acids Research*, *50*(W1), W330-W336. https://doi.org/10.1093/nar/gkac441

Maharramov, E., Czikkely, M. S., Szili, P., Farkas, Z., Grézal, G., Daruka, L., Kurkó, E., Mészáros, L., Daraba, A., Kovács, T., Bognár, B., Juhász, S., Papp, B., Lázár, V., & Pál, C. (2025). Exploring the principles behind antibiotics with limited resistance. *Nature Communications*, *16*(1). https://doi.org/10.1038/s41467-025-56934-3

Qazi, S. N. A., Counil, E., Morrissey, J., Rees, C. E. D., Cockayne, A., Winzer, K., Chan, W. C., Williams, P., & Hill, P. J. (2001). agr Expression Precedes Escape of Internalized

Staphylococcus aureus from the Host Endosome. *Infection and Immunity*, *69*(11), 7074-7082. https://doi.org/10.1128/iai.69.11.7074-7082.2001

Darch, S. E., West, S. A., Winzer, K., & Diggle, S. P. (2012). Density-dependent fitness benefits in quorum-sensing bacterial populations. *Proceedings of the National Academy of Sciences*, *109*(21), 8259-8263. https://doi.org/10.1073/pnas.1118131109

Langmead, B., & Salzberg, S. L. (2012). Fast gapped-read alignment with Bowtie 2. *Nature Methods*, *9*(4), 357-359. https://doi.org/10.1038/nmeth.1923

Bolger, A. M., Lohse, M., & Usadel, B. (2014). Trimmomatic: a flexible trimmer for Illumina sequence data. *Bioinformatics*, *30*(15), 2114-2120. https://doi.org/10.1093/bioinformatics/btu170

Li, H., Handsaker, B., Wysoker, A., Fennell, T., Ruan, J., Homer, N., Marth, G., Abecasis, G., & Durbin, R. (2009). The Sequence Alignment/Map format and SAMtools. *Bioinformatics*, *25*(16), 2078-2079. https://doi.org/10.1093/bioinformatics/btp352

Liao, Y., Smyth, G. K., & Shi, W. (2014). featureCounts: an efficient general purpose program for assigning sequence reads to genomic features. *Bioinformatics*, *30*(7), 923-930. https://doi.org/10.1093/bioinformatics/btt656

Love, M. I., Huber, W., & Anders, S. (2014). Moderated estimation of fold change and dispersion for RNA-seq data with DESeq2. *Genome Biology*, *15*(12). https://doi.org/10.1186/s13059-014-0550-8

Leggett, R. M., Ramirez-Gonzalez, R. H., Clavijo, B. J., Waite, D., & Davey, R. P. (2013). Sequencing quality assessment tools to enable data-driven informatics for high throughput genomics. *Frontiers in Genetics*, *4*. https://doi.org/10.3389/fgene.2013.00288

R Core Team (2023). R: A Language and Environment for Statistical Computing. R Foundation for Statistical Computing, Vienna, Austria. https://www.R-project.org/

Righetti, K. M. (2011). Study of Rsm/Gac post-transcriptional regulation by quorum sensing, extracellular and intracellular signals in *Pseudomonas aeruginosa*. PhD thesis, University of Nottingham.